ELSEVIER

Colloids and Surfaces
A: Physicochemical and Engineering Aspects 173 (2000) 127–158

COLLOIDS AND SURFACES A

www.elsevier.nl/locate/colsurfa

Acoustic and electroacoustic spectroscopy

A.S. Dukhin [a], P.J. Goetz [a], T.H. Wines [b], P. Somasundaran [b,*]

[a] *Dispersion Technology Inc., 3 Hillside Avenue, Mt Kisco, NY 10549, USA*
[b] *Columbia University, Rm. 911, 500 W. 120th Street, 1140 Amsterdam Avenue, New York, NY 10027, USA*

Received 28 September 1999; accepted 13 March 2000

Abstract

Two new ultrasound based techniques (acoustics and electroacoustics) offer a unique opportunity to characterize concentrated dispersion, emulsions and microemulsions in their natural state, without dilution. Elimination of the dilution protocol is crucial for an adequate characterization of liquid dispersions, especially structured. Dilution changes the thermodynamic equilibrium in these systems and affects their reological properties. Changes in equilibrium conditions can lead to variation of the particle size and can also affect surface chemistry. In this paper, a short review of the theoretical basis of the ultrasound techniques is given. Emphasis is placed on the theoretical models which are supposed to be valid in concentrated systems. These theories have been developed recently on the basis of 'cell model concept' for both acoustics and electroacoustics. This approach opens the way to implement particle–particle interaction into the theoretical model. Experiment proves that these theories are adequate in concentrated systems up to 45% vol. Second part of the paper is dedicated to the applications of acoustics and electroacoustics. The list of applications includes: ceramics, mixed dispersed systems, chemical-polishing materials, emulsions, food emulsions, microemulsions and latecies.

Keywords: Acoustic spectroscopy; Electroacoustic spectroscopy; Ultrasound techniques

. Introduction

The widespread acceptance and commercialization of acoustic spectroscopy has been slow to develop. This technique has been overlooked by many in academia and industry in the past, but has recently been showing increased levels of acceptance. This powerful method of characterizing concentrated heterogeneous systems has all the capabilities for being successful. The first hardware for measuring acoustic properties of liquids was developed more than 50 years ago at MIT [1] by Pellam and Galt. The first acoustic theory for heterogeneous systems was created by Sewell 90 years ago [2]. The general principles of the acoustic theory were formulated 45 years ago by Epstein and Carhart [3]. There is a long list of applications and experiments using acoustic spectroscopy, see reviews [4,5]. Despite all of these developments, however, acoustic spectroscopy is rarely mentioned in modern handbooks on colloid science [6,7].

* Corresponding author. Tel.: +1-212-8542926; fax: +1 212-8548362.
E-mail address: ps24@columbia.edu (P. Somasundaran).

0927-7757/00/$ - see front matter
PII: S0927-7757(00)00593-8

Acoustics is able to provide reliable particle size information for concentrated dispersions without any dilution. There are examples when acoustics yields size information at volume fractions above 40%. This in-situ characterization of concentrated systems makes the acoustic method very useful and unique in this capability compared to alternate methods including light scattering where dilution is required. Acoustics is also able to deal with low dispersed phase volume fractions and in some systems can characterize down to below 0.1% vol. This flexibility for concentration range provides an overlap with classic methods for dilute systems. In the overlap range, acoustics size characterization has been found to have excellent agreement with these other techniques.

Acoustics is not only a particle sizing technique, but also provides information about the microstructure of the dispersed system. The acoustic spectrometer can be considered as a micro-rheometer. In acoustics, stresses are applied in the same way as regular rheometers, but over a very short distances on the micron scale. In this way, the microstructure of the dispersed system can be sensed. Currently, this feature of the acoustics is only beginning to be exploited, but it is certainly very promising.

Many people have perceived acoustics to have a high degree of complexity. The operating principles are in fact quite straightforward. The acoustic spectrometer generates sound pulses that pass through a sample system and are then measured by a receiver. The passage through the sample system causes the sound energy to change in intensity and phase. The acoustic instrument measures the sound energy losses (attenuation) and the sound speed. The sound attenuates due to the interaction with the particles and liquid in the sample system, Acoustic spectrometers generally operate with sound in the frequency range of 1–100 MHz. This is a much higher sound frequency than the upper limit of the hearing which is only 0.02 MHz.

While the operating principles are relatively simple, the analysis of the attenuation data to obtain particle size distributions does involve a degree of complexity in fitting experimental results to theoretical models based on various acoustic loss mechanisms. The advent of high speed computers and the refinement of these theoretical models has made the inherent complexity of this analysis of little consequence. In comparison, many other particle sizing techniques such as photon correlation spectroscopy also rely on similar levels of complexity in analyzing experimental results.

Acoustics has a related field that is usually referred to as 'electroacoustics' [8]. Electroacoustics can provide particle size distribution as well as ζ-potential. This relatively new technique is more complex than acoustics because an additional electric field is involved. As a result, both hardware and theory become more complicated. There are even two different versions of electroacoustics depending on what field is used as a driving force. Electrokinetic sonic amplitude (ESA) involves the generation of sound energy caused by the driving force of an applied electric field. Colloid vibration current (CVI) is the phenomenon where sound energy is applied to a system and a resultant electric field or current is created by the vibration of the colloid electric double layers.

Coming back to acoustics, it's lack of widespread acceptance may be related to the fact that it yields too much, sometimes overwhelming information. Instead of dealing with interpretation of the acoustic spectra it is often easier to dilute the system of interest and apply light based techniques. It was often naively assumed that the dilution had not affected the dispersion characteristics. Lately, many researchers are coming to the realization that dispersed systems need to be analyzed in their natural concentrated form, and that dilution destroys a lot of useful and important properties.

The authors are optimistic about the future of acoustics in colloid science. It is amazing what this technique can do especially in combination with electroacoustics for characterizing electric surface properties. It is hoped that this review will allow one to taste the power and opportunities related to these sound based techniques.

2. Theoretical background

There are six known mechanisms of the ultrasound interaction with a dispersed system: (1) viscous (α_{vis}); (2) thermal (α_{th}); (3) scattering (α_{sc}); (4) intrinsic (α_{int}); (5) structural (α_{str}); and (6) electrokinetic (α_{ele}).

(1). The viscous losses of the acoustic energy occur due to the shear waves generated by the particle oscillating in the acoustic pressure field. These shear waves appear because of the difference in the densities of the particles and medium. This density contrast causes the particle motion with respect to the medium. As a result, the liquid layers in the particle vicinity slide relative to each other. This sliding non-stationary motion of the liquid near the particle is referred to as the 'shear wave'. Viscous losses are dominant for small rigid particles with sizes below 3 μm, such as oxides, pigments, paints, ceramics, cement, graphite, etc.

(2). The reason for the thermal losses is the temperature gradients generated near the particle surface. These temperature gradients are due to the thermodynamic coupling between pressure and temperature. This mechanism is dominant for soft particles, including emulsion droplets and latex beads.

(3). The mechanism of the scattering losses is quite different than the viscous and thermal losses. Acoustic scattering does not produce dissipation of acoustic energy. This scattering mechanism is similar to light scattering. Particles simply redirect a part of the acoustic energy flow and as a result this portion of the sound does not reach the sound transducer. This mechanism is important for larger particles (>3 μm) and high frequency (>10 MHz).

(4). The intrinsic losses of the acoustic energy occur due to the interaction of the sound wave with the materials of the particles and medium as homogeneous phases on a molecular level.

(5). Structural losses are caused by the oscillation of a network of particles that are interconnected. Thus, this mechanism is specific for the given type of structured system.

(6). Electrokinetic losses are caused by the oscillation of charged particles in an acoustic field that leads to the generation of an alternating electrical field, and consequently to alternating electric current. As a result, a part of the acoustic energy is transformed into electric energy and then irreversibly to heat.

Only the first four loss mechanisms (viscous, thermal, scattering and intrinsic) make a significant contribution to the overall attenuation spectra in most cases. Structural losses are significant only in structured systems that require a quite different theoretical framework. These four mechanisms form the basis for acoustic spectroscopy. Total attenuation measured with acoustic spectrometer usually equals to the sum of these four partial attenuations:

$$\alpha = \alpha_{vis} + \alpha_{th} + \alpha_{sc} + \alpha_{int} \quad (1)$$

The contribution of electrokinetic losses to the total sound attenuation is almost always negligibly small [9] and will be neglected. This opens an opportunity to separate acoustic spectroscopy from electroacoustic spectroscopy because acoustic attenuation spectra is independent of the electric properties of the dispersed system.

Following this distinction between acoustics and electroacoustics, the corresponding theories will be considered separately.

2.1. Theory of acoustics

The most well known acoustic theory for heterogeneous systems was developed by Epstein and Carhart [3], Allegra and Hawley [10]. This theory takes into account the four most important mechanisms (viscous, thermal, scattering and intrinsic) and is termed the 'ECAH theory'. This theory describes attenuation for a monodisperse system of spherical particles and is valid only for dilute systems.

The term 'monodisperse' assumes that all of the particles have the same diameter. Extensions of the ECAH theory to include polydispersity have typically assumed a simple linear superposition of the attenuation for each size fraction. The term 'spherical' is used to denote that all calculations are performed assuming that each particle can be adequately represented as a sphere.

Most importantly, the term 'dilute' is used to indicate that there is no consideration of particle–

particle interactions. This fundamental limitation normally restricts the application of the resultant theory to dispersions with a volume fraction of less than a few volume percent. However, there is some evidence that the ECAH theory, in some very specific situations, does nevertheless provide a correct interpretation of experimental data, even for volume fractions as large as 30%.

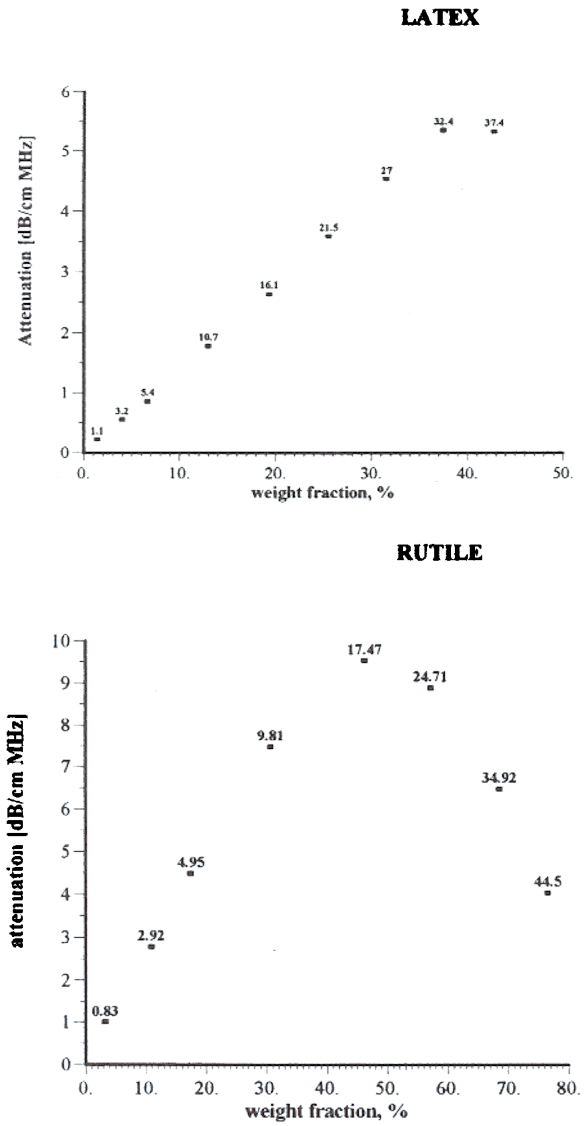

Fig. 1. Dependence of the attenuation in the neoprene latex and in the rutile dispersion (rutile R-746 by DuPont) at the frequency 15 MHz on the dispersed system weight fraction. Corresponding volume fractions in % are shown as the data points labels.

An early demonstration of the ability of the ECAH theory was provided by Allegra and Hawley. They observed almost perfect correlation between experiment and dilute case ECAH theory for several systems: a 20% by volume toluene emulsion; a 10% by volume hexadecane emulsion; and a 10% by volume polystyrene latex. Similar work with emulsions by McClements [11,12] has provided similar results. The recent work by Holmes, Challis and Wedlock [13,14] shows good agreement between ECAH theory and experiments even for 30% by volume polystyrene latex.

A surprising absence of particle–particle interaction was observed with neoprene latex [15]. This experiment showed that attenuation is linear function of the volume fraction up to 30% for this particular system (Fig. 1). This linearity is an indication that each particle fraction contributes to the total attenuation independently of other fractions, and is a superposition of individual contributions. Superposition works only when particle–particle interaction is insignificant.

It is important to note that the surprising validity of the dilute ECAH theory for moderately concentrated systems has only been demonstrated in systems where the 'thermal losses' were dominant, such as emulsions and latex systems. In contrast, the solid rutile dispersion exhibits nonlinearity of the attenuation above 10% by volume (Fig. 1).

The difference between the 'viscous depth' and the 'thermal depth' provides an answer to the observed differences between emulsions and solid particle dispersions. These parameters characterize the penetration of the shear wave and thermal wave correspondingly into the liquid. Particles oscillating in the sound wave generate these waves which damp in the particle vicinity. The characteristic distance for the shear wave amplitude to decay is the 'viscous depth' δ_v. The corresponding distance for the thermal wave is the 'thermal depth' δ_t. The following expressions give these parameters values in the dilute systems:

$$\delta_v = \sqrt{\frac{2\nu}{\omega}} \tag{2}$$

$$\delta_t = \sqrt{\frac{2\tau_m}{\omega\rho_m C_p^m}} \quad (3)$$

where ν is the kinematic viscosity, ω is the frequency, ρ_m is the density, τ_m is heat conductance, C_p^m is a heat capacity at constant pressure of liquid.

The relationship between δ_ν and δ_t has been considered before. For instance, McClements plots 'thermal depth' and 'viscous depth' versus frequency [4]. It is easy to show that 'viscous depth' is 2.6 time more than 'thermal depth' in aqueous dispersions [15]. As a result, the particle viscous layers overlap at the lower volume fraction more than the particle thermal layers. Overlap of the boundary layers is the measure of the corresponding particle–particle interaction. There is no particle interaction when corresponding boundary layers are sufficiently separated.

Thus, an increase in the dispersed volume fraction for a given frequency first leads to the overlap of the viscous layers because they extend further into the liquid. Thermal layers overlap at higher volume fractions. This means that the particle hydrodynamic interaction becomes more important at the lower volume fractions than the particle thermodynamic interaction.

The 2.6 times difference between δ_ν and δ_t leads to a big difference in the volume fractions corresponding to the beginning of the boundary layers overlap. The dilute case theory is valid for the volume fractions smaller than these critical volume fractions φ_ν and φ_t. These critical volume fractions, φ_ν and φ_t are functions of the frequency and particle size. These parameters are conventionally defined from the condition that the shortest distance between particle surfaces is equal to 2 δ_ν or 2 δ_t. This definition gives the following expression for the ratio of the critical volume fractions in aqueous dispersions:

$$\frac{\varphi_\nu}{\varphi_t} = \left(\frac{a\sqrt{\pi f} + 2.6^{-1}}{a\sqrt{\pi f} + 1}\right)^3 \quad (4)$$

where a is particle radius in micron, f the frequency is in MHz.

The ratio of the critical volume fractions depends on the frequency. For instance for neoprene latex, the critical 'thermal' volume fraction is 10 times higher than the critical 'viscous' volume fraction for 1 MHz and only 3 times higher for 100 MHz.

It is interesting that this important feature of the 'thermal losses' works for almost all liquids. There is more than 100 liquids with their properties in the database. The core of this database is the well known paper by Anson and Chivers [16]. A parameter referred to as 'depth ratio' can be introduced

$$\text{depth ratio} = \frac{\delta_\nu}{\delta_t}$$

This parameter is 2.6 for water as was mentioned before. Fig. 2 shows values of this parameter for all liquids from the database relative to the viscous depth of water. It is seen that this parameter is even larger for many liquids.

Therefore 'thermal losses' are much less sensitive to the particle–particle interaction than 'viscous losses' for almost all known liquids. It makes ECAH theory valid in a much wider range of emulsion volume fractions than one would expect.

There is one more fortunate fact for ECAH theory that follows from the values of the liquid's thermal properties. In general, ECAH theory requires information about three thermodynamic properties: thermal conductivity τ, heat capacity C_p and thermal expansion β. It turns out that τ and C_p are almost the same for all liquids except water. Fig. 3 illustrate variation of these parameters for more than 100 liquids from the database. This reduces the number of required parameters to one-thermal expansion. This parameter plays the same role in 'thermal losses' as density in 'viscous losses'.

ECAH theory has a big disadvantage of being mathematically complex. It cannot be generalized for particle–particle interactions. This is not important as has been found for emulsions, but may be important for latex systems, and is certainly very important for high density contrast systems. There are two ways to simplify this theory using a restriction on the frequency and particle size. The first one is the so called 'long wave requirement' [10] which requires the wave length of the sound wave λ to be larger than particle radius a. This 'long wave requirement' restricts particle size for a given set of frequencies. The authors' experience

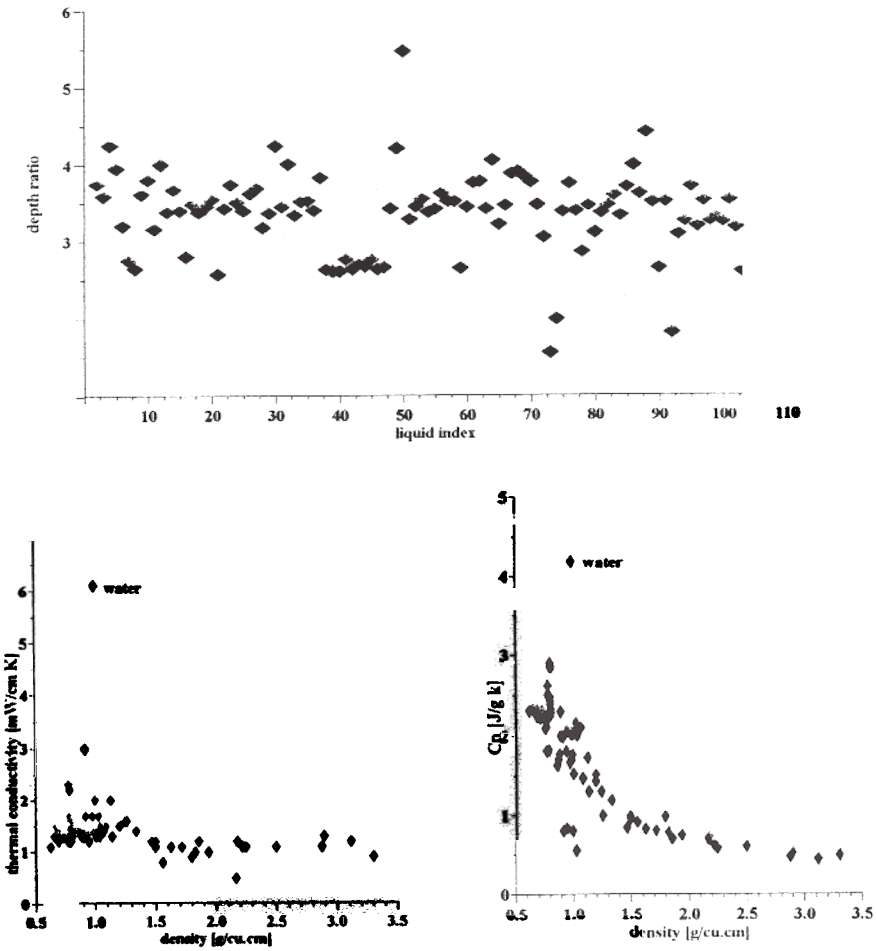

Fig. 2. Thermal properties of various liquids.

shows that particle size must be below 10 μm for the frequency range from 1 to 100 MHz. This restriction is helpful for characterizing small particles.

By restricting frequency and particle size with the longwave requirement one can use the simpler explicit expression for the thermal losses α_{th} obtained initially by Isakovich [17] and confirmed later by Epstein and Carhart [3], and Allegra and Hawley [10]:

$$\alpha_{th} = \frac{3\varphi T c_m \rho_m \tau_m}{2a^2}\left(\frac{\beta_m}{\rho_m C_p^m} - \frac{\beta_p}{\rho_p C_p^p}\right)^2 \mathrm{Re}\left(\frac{1}{1-jz_m} - \frac{\tau_m \tanh z_p}{\tau_p \tanh z_p - z_p}\right) \quad (5)$$

where

$$z = (1+j)a\sqrt{\frac{\omega \rho C_p}{2\tau}}$$

where j is imagine number, φ is the volume fraction, T is the absolute temperature, ω is the angular frequency, c is the sound speed, ρ is the density, τ is the thermal conduction, β is thermal expansion, C_p is specific heat at the constant pressure. Index m corresponds to the medium whereas index p indicates particles.

At the same time the long wave requirement provides a sufficient simplification of the theory for implementing particle–particle hydrodynamic interaction into the theory of the viscous losses. It has been done in the work [18] on the basis of the 'coupled phase model' [19,20]. This new theory [21] works up to 40% volume.

This theory yields expression for the complex wavenumber l assuming viscous losses as the only one mechanism of the particles interaction with the sound wave:

$$\frac{l^2M^*}{\omega^2}=\frac{\rho_m(1-\varphi)+\rho_p\sum_{i=1}^{N}\frac{\varphi_i\gamma_i}{j\omega\rho_p\varphi_i+\gamma_i}}{(1-\varphi)^2+\sum_{i=1}^{N}\frac{\varphi_i(\varphi-2)\gamma_i-\varphi_i^2(1-\varphi)\rho_m}{j\omega\rho_p\varphi_i-\gamma_i}} \quad (6)$$

where

$$\gamma=\frac{9\eta\varphi\Omega}{2a^2}$$

$$F_f=6\pi\eta a\Omega(u_p-u_m)$$

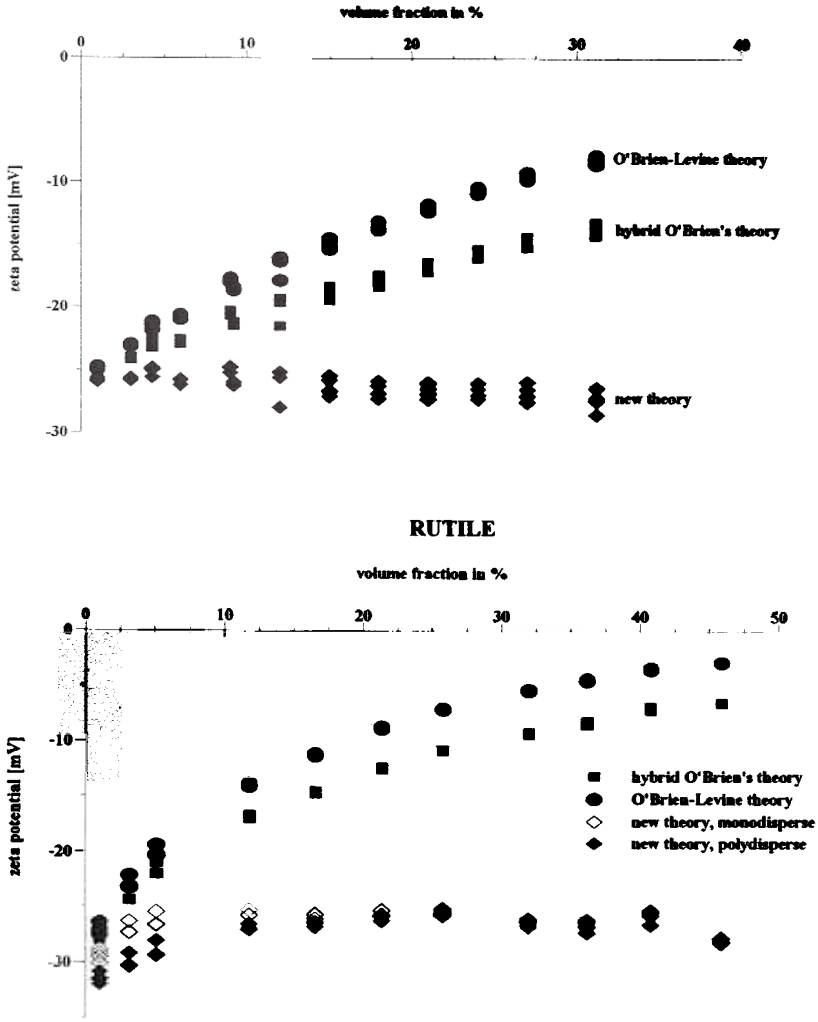

Fig. 3. Electrokinetic ζ-potential calculated from the measured colloid vibration current (CVI) at various volume fractions using different electroacoustic theories for silica Ludox and for rutile R-746 from Dupont.

η is dynamic viscosity, u_p and u_m are velocities of the particles and liquid in the laboratory frame of references, Ω is drag coefficient specified in Appendix A, M^* is stress modulus which can be expressed in terms of densities and sound speeds as following:

$$M^* = \frac{\rho_p \rho_m c_p^2 c_m^2}{\varphi \rho_m c_m^2 + (1-\varphi)\rho_p c_p^2}$$

Expression (6) specifies the value of viscous losses:

$$\alpha_{vis} = -\mathrm{Im} l \tag{7}$$

This theory can be used also for calculating sound speed of the dispersions where viscous losses are dominant.

$$c_s = \frac{\omega}{\mathrm{Re} l} \tag{8}$$

Experiment described in papers [22,23] confirms validity of this theory for sound speed.

Expressions for calculating intrinsic α_{int} and scattering α_{sc} losses for long wave limit are given in the papers of McClements [4,11,12,24]. He uses term 'lossless scatterers' for describing sound propagation through the system when dissipative mechanisms of viscous and thermal losses are negligible. Intrinsic attenuation in such a system can be expressed as following [15]:

$$\alpha_{int} = \frac{(1-\varphi)\frac{\alpha_m}{c_m} + \varphi \frac{\rho_m \alpha_p}{\rho_p \alpha_m}}{\sqrt{\frac{1-\varphi}{c_m^2} + \frac{\varphi \rho_m}{\rho_p c_p^2}}} \sqrt{\frac{\rho_s}{\rho_m}} \tag{9}$$

where α_m and α_p are attenuations of the medium and particle materials.

Scattering attenuation can be calculated following Waterman–Truell [24] theory which yields the following expression for the complex wavenumber l_s associated with scattering:

$$\frac{l_s^2}{l_m^2} = \left(1 - \frac{3j\varphi}{(l_m a)^3} A_0\right)\left(1 - \frac{9j\varphi}{(l_m a)^3} A_1\right)$$

where A_0 and A_1 are monopole and dipole scattering coefficients calculated for a single particle,

$$l_s = \frac{\omega}{c_s} + j\alpha_{sc}$$

$$l_m = \frac{\omega}{c_m} + j\alpha_m$$

The simplest formula expressing the scattering losses in terms of densities and sound speeds can be derived from Eq. (9) for a single scattering:

$$\alpha_{sc} = \frac{\varphi \omega^4 a^3}{2c_m^4}\left[\frac{1}{3}\left(1 - \frac{\rho_m c_m^2}{\rho_p c_p^2}\right)^2 + \left(\frac{\rho_p - \rho_m}{2\rho_p + \rho_m}\right)^2\right] \tag{10}$$

It is seen that scattering losses depend on frequency very strongly. According to the authors' experience scattering is important only for large particle (> 3 μm) and at high frequencies (> 10 MHz).

There is another approach to acoustics which employs a 'short wave requirement'. It was introduced by Riebel [21]. This approach works only for large particles above 10 μm and requires limited input data about the sample. This theory may provide an important advantage in the case of emulsions and latex systems when the thermal expansion is not known.

There is opportunity in the future to create a mixed theory that could use a polynomial fit merging together 'short' and 'long' wave ranges theories. Such combined theory will be able to cover a complete particle size range from nanometers to millimeters for concentrated systems.

There are two recent developments in the theory of acoustics which deserved to be mentioned here. The first one is a theory of acoustics for flocculated emulsions [25]. It is based on ECAH theory but it uses in addition an 'effective medium' approach for calculating thermal properties of the flocs. The success of this idea is related to the feature of the thermal losses that allows for insignificant particle–particle interactions even at high volume fractions. This mechanism of acoustic energy dissipation does not require relative motion of the particle and liquid. Spherical symmetrical oscillation is the major term in these types of losses. This provides the opportunity to replace the floc with an imaginary particle assuming a proper choice of the thermal properties.

Another significant recent development is associated with the name of Samuel Temkin. He offers in his recent papers [26,27] a new approach to the acoustic theory. Instead of assuming a model

dispersion consisting of spherical particles in a Newtonian liquid, he suggests that the thermodynamic approach be explored as far as possible. This new theory operates with notions of particle velocities and temperature fluctuations. This very promising theory yields some unusual results [26,27]. It has not been yet used, as far as is known, in commercially available instruments.

2.2. Theory of electroacoustics

Whereas acoustic spectroscopy describes the combined effect of the six separate loss mechanisms, electroacoustic spectroscopy, as it is presently formulated, emphasizes only one of these interaction mechanisms, the electrokinetic losses.

In acoustic spectroscopy sound is utilized as both the excitation and the measured variable, and therefore there is but one basic implementation. In contrast, electroacoustic spectroscopy deals with the interaction of electric and acoustic fields and therefore there are two possible implementations. One can apply a sound field and measure the resultant electric field which is referred to as the colloid vibration potential (CVP), or conversely one can apply an electric field and measure the resultant acoustic field which is referred to as the electronic sonic amplitude (ESA).

First let one consider the measurement of CVP. When the density of the particles ρ_p differs from that of the medium ρ_m, the particles move relative to the medium under the influence of an acoustic wave. This motion causes a displacement of the internal and external parts of the double layer (DL). This phenomenon is usually referred to as a polarization of the DL [6]. This displacement of opposite charges gives rise to a dipole moment. The superposition of the electric fields of these induced dipole moments over the collection of particles gives rise to a macroscopical electric current which is referred to as the colloid vibration current (CVI). Thus, the fourth mechanism of particles interaction with sound leads to the transformation of part of the acoustic energy to the electric energy. This electric energy may then be dissipated if the opportunity for the electric current flow exists.

Now let one consider the measurement of ESA which occurs when an alternating electric field is applied to the disperse system [7]. If the ζ-potential of the particle is greater than zero, then the oscillating electrophoretic motion of the charged dispersed particles generates a sound wave.

Both electroacoustic parameters CVI and ESA can be experimentally measured. The CVI or ESA spectrum is the experimental output from electroacoustic spectroscopy. Both of these spectra contain information about ζ-potential and PSD, however, only one of the electroacoustic spectra is required because both of them contain essentially the same information about the dispersed system.

The conversion electroacoustic spectra into the PSD requires theoretical model of the electroacoustic phenomena. This conversion procedure is much more complicated for electroacoustics comparing to the acoustics. The reason of the additional problems relates to the additional field involved in the characterization: electric field. The theory becomes much more complicated because of this additional field.

For some time O'Brien's theory [28,29] has been considered as a basis for electroacoustics including concentrated systems. This theory introduces a notion of dynamic electrophoretic mobility μ_d. It declares that CVI and/or ESA are proportional to this parameter with coefficient which is independent on frequency and particle size:

$$\mathrm{ESA(CVI)} = C_{\mathrm{cal}} \frac{\rho_p - \rho_m}{\rho_m} \varphi \mu_d E(\nabla P) \qquad (11)$$

where C_{cal} is a cell constant, P is the hydrodynamic pressure, and E is the external electric field strength.

One can see that according to the O'Brien's theory electrophoretic dynamic mobility contains all information about particle size and ζ-potential. It makes this parameter a key for electroacoustic theory. The most promising theory of the dynamic electrophoretic mobility has been created recently by Ohshima, Dukhin and Shilov [30,22,31].

Unfortunately it turned out that situation with electroacoustic theory is more complicated than predicted by O'Brien's theory. It was shown re-

cently that O'Brien's theory relationship (Eq. (11)) contradicts the Onsager principle and Smoluchowski theory if applied for concentrated systems. This conclusion was confirmed experimentally with the two equilibrium dilution tests performed with small silica (30 nm) and larger rutile (300 nm). Results of this experiment are shown on Fig. 3. Term 'hybrid O'Brien's theory' corresponds to the combination of the O'Brien's relationship (Eq. (11)) and Ohshima–Dukhin–Shilov cell model [30,22,31].

Test with the small silica Ludox is the most impressive because cell model theory reduces to the Smoluchowski law in this case. Assumptions of the cell model does not affect theoretical results in this case and yet there is a big discrepancy between O'Brien theory and experiment. It proves that the reason of the theory failure is expression (11).

It turned out that coefficient between electroacoustic signal (CVI or ESA) and dynamic mobility depends on frequency and particle. It diminishes importance of the dynamic mobility because there is no simple way to calculate it from the electroacoustic signal.

There is another electroacoustic theory created in the work [23] without using O'Brien relationship. It yields the following expression for CVI:

$$\mathrm{CVI} = \frac{9\varepsilon\varepsilon_0\zeta(1-\varphi)(\rho_p-\rho_m)\omega\nabla P}{4(1+0.5\varphi)\eta(1-\varphi)} \frac{\sum_{i=1}^{N}\frac{\varphi_i h(\alpha_i)}{\alpha_i I(\alpha_i)\left(j\omega\rho_p+\frac{\gamma_i}{\varphi_i}\right)}}{+\frac{\rho_p}{(1-\varphi)\rho_m}\sum_{i=1}^{N}\frac{\gamma_i}{j\omega\rho_p+\frac{\gamma_i}{\varphi_i}}}$$

$$\alpha_i = \frac{a_i\sqrt{\omega\rho_m}}{\sqrt{2\eta}}$$

where ε and ε_0 are dielectric permittivities of the medium and vacuum, h and I are special function given in Appendix A as well as drag coefficient γ.

This new theory has been tested experimentally (Fig. 3). It is seen that theory works up to 45% vol. because it produces ζ-potential which is almost independent on volume fraction. It is supposed to be this way because dilution tests were performed using equilibrium supernate. This supernate was generated for silica with dialysis, and for rutile with centrifugation.

So far, this new electroacoustic theory has been tested with rigid heavy particles only. It is not clear yet how it will work for emulsions as there were no experimental data with emulsions available. This concern is related to the fact that this new theory as well as O'Brien's theory neglect thermodynamic effects. It is rather surprising keeping in mind that the thermodynamic effect of 'thermal losses' is dominant for acoustics of emulsions. It is not clear yet why electroacoustics is so different from acoustics in that thermodynamic effects are not important.

One simple hypothesis is offered which might explain this difference. Electroacoustics is related to the displacement of the electric charges in the double layer (DL). This displacement is characterized by dipole symmetry. At the same time 'thermal losses' measured by acoustics are associated mostly with spherical symmetry. They are caused by oscillation of the particle's volume in the sound wave. It is clear that such a spherically symmetrical oscillation does not cause displacement of electric charges in the DL with dipole structure.

This is a hypothesis and a fundamental theory that will take into account thermodynamic effects in addition to electrodynamic and hydrodynamic effects should resolve this question. The electroacoustic theory of emulsions will not be complete unless such a theory is developed.

Nevertheless, electroacoustics even at present stage can yield very important information about electric surface properties of emulsions as it will be shown below.

2.3. Bubbles problem

One of the experimental problems that may affect acoustics is the presence of air bubbles during measurements. While bubbles will affect sound attenuation and speed, it is worth considering how much of an effect they really have and whether the bubbles will detract from the acoustic techniques:

1. It has been determined that acoustic spectra is affected by bubbles. An acoustic theory describing sound propagation through bubbly liquid has been created by Foldy in 1944 [32], and confirmed experimentally in 1940–1950 [33–35].
2. Contribution of bubbles to sound speed and attenuation depends on the bubble size and sound frequency. For instance, a 100 μm bubble has a resonance frequency of about 60 KHz. This frequency is reciprocally proportional to the bubble diameter. A bubble of 10 μm diameter will have a resonance frequency of about 0.6 MHz.
3. Acoustic spectroscopy of dispersed systems operates with frequencies above 1 MHz and usually up to 100 MHz. The size of the bubbles must be well below 10 μm in order to affect the complete frequency range of acoustic spectrometer.
4. Bubbles with sizes below 10 μm are very unstable as is known from general colloid chemistry and the theory of flotation. 'Colloid-sized gas bubbles have astonishingly short lifetimes, normally between 1 μs and 1 ms'. [35]. They simply dissolve in liquid because of high curvature.

Bubbles can only affect the low frequency part of the acoustic spectra below 10 MHz. The frequency range from 10 to 100 MHz is available for particle characterization even in the bubbly liquids. Acoustic spectrometer can do both, sense bubbles and characterize particle size. This conclusion can be confirmed with thousands of measurements performed with hundreds of different systems. Sensitivity to bubbles, in fact, is an important advantage of acoustics over electroacoustrics. The presence of bubbles may affect the properties of the solid dispersed phase. For instance, bubbles can be centers of aggregation which makes them an important stability factor.

3. Measuring technique

Currently, there are three acoustic spectrometers on the market: Ultrasizer of Malvern, Opus of Sympatec and DT-100 of Dispersion Technology. All of them claim to be able to characterize emulsions in the wide droplet size range. There are some major differences between them. For instance Opus was designed initially for large particles only because it employs the 'short wavelength requirement' [25].

There are also three electroacoustic spectrometers on the market: Matec ESA 9800, the Acoustosizer of Colloidal Dynamics and the DT-200 of Dispersion Technology.

There is only one instrument which provides both features, acoustics and electroacoustics together, and this is the DT-1200 Acoustic and Electroacoustic Spectrometer of Dispersion Technology.

Comparison of the different instruments lies beyond the scope of this review. The DT-1200 was used for all experiments described in this work. A description of this instrument is given in the papers [23,36–38] including accuracy and precision tests.

There is one more recent development made by Dispersion Technology, which might be of the big interest, especially for on-line measurements and routine quality control. It is electroacoustic probe described in details in the pending patent [38]. This probe implements a completely new method of characterizing particle size and ζ-potential which is based on the new electroacoustic theory [23] for concentrated colloids. This probe measures CVI as well as DT-1200. The difference is that sensing electric electrode is placed on the surface of the ultrasound transducer. This design eliminates contribution of attenuation. Sample volume is much smaller, probe diameter is about 3 cm only. It can be easily immersed into the small sample container. In addition, it makes possible to characterize colloids on-line.

4. Applications

4.1. Ceramics

Determination of both the particle size distribution and the ζ-potential of ceramic slurries is of key importance in optimizing performance. The particle size of the slip is closely related to inho-

mogeneities, which in turn relate to fracture origins as well as shape distortion/cracking during drying, pyrolysis and sintering. Furthermore, the ζ-potential of the slurry particulates can be used as a tool for optimizing chemical dosage to achieve the desired colloid stability and size distribution.

Traditional measurements of particle size and ζ-potential usually involve light scattering or sedimentation techniques and require extreme dilution of the ceramic slip. This dilution step often changes both the size distribution and the ζ-potential of the sample, thereby distorting the very information being sought. Characterizing the concentrated sample directly would allow one to realistically judge the true agglomeration status of the slip and to optimize the dosage of various chemical additives in situ. In contrast, measurements of the diluted samples with traditional methods often reveal only the primary size of the raw materials since the usual sample preparation steps of dilution, chemical modification, stirring and perhaps even sonication have destroyed most of the useful information about the original slurry.

Acoustic spectroscopy can provide accurate particle size data even in concentrated slurries. Fig. 4 shows the measured attenuation spectra and corresponding particle size distribution for four different alumina slurries. Table 1gives a comparison of the measured particle size with the manufacturer's data derived from traditional methods.

The agreement between acoustic and traditional methods is quite good because care was taken in formulating the concentrated dispersion with an optimum level of surfactant to insure good dispersion of the primary particles. In many real-world cases, the final dispersant dose may have been simply extrapolated from very dilute measurements and one may obtain a larger particle size in the actual slurry than predicted from these dilute measurements of the raw materials. It is almost always better to characterize the particle size of the slurry. When this does not compare with dilute measurements one needs to examine whether the chemical formulation is adequate.

Acoustic spectroscopy is applicable to virtually all ceramic materials. Fig. 5 shows typical particle size distributions for a variety of commonly used ceramic materials.

For many applications it is important to recognize particle size sub-populations in the final slurry. Such bimodal distributions might result from agglomeration of primary particles caused by non-optimum dispersant addition, or in the following example, from an intentional addition of a second size fraction. Fig. 6 shows the acoustic attenuation spectra for three 10 vol.% alumina slurries: a 0.36 μm sample, a 2 μm sample, and a 1:1 mix of the two. The theoretical spectra fit quite precisely the experimental data giving high confidence in the results. Fig. 6 shows the resulting size distributions for the two single component slurries (blue and black curves) as well as the bimodal distribution for the mixed slurry (red curve).

In many ceramic applications the ceramic slip is actually a mixture of more than one solid component. Traditional optical or sedimentation techniques can not provide correct interpretation of such mixtures and typically assume that all particles have a common set of physical properties. In contrast, commercially available software for acoustic spectroscopy has evolved to the point that allows the specification of at least two classes of disperse particles. For example, Fig. 7 shows an example of a mixed system of alumina and zirconia particles. This Figure shows the attenuation spectra for three 5 vol.% slurries: a 2 μm single component alumina, a 0.3 μm single component zirconia, and a 1:1 mix of the two ingredients. Again, the theoretical spectra fit the experimental data quite precisely giving high confidence in the results. Fig. 7 shows the resulting single mode particle size distribution for each oxide measured separately, as well as two separate single mode distributions measured for each component in the mixed slurry system.

It is not always appreciated that the particle size distribution of a slurry is not simply a function of the primary size of the constituent ingredients, but instead is a result of many complex chemical and mechanical operations on the system. The ζ-potential of the system is one parameter that can be used to investigate this complex relationship. Fig. 8 compares ζ-potential data for

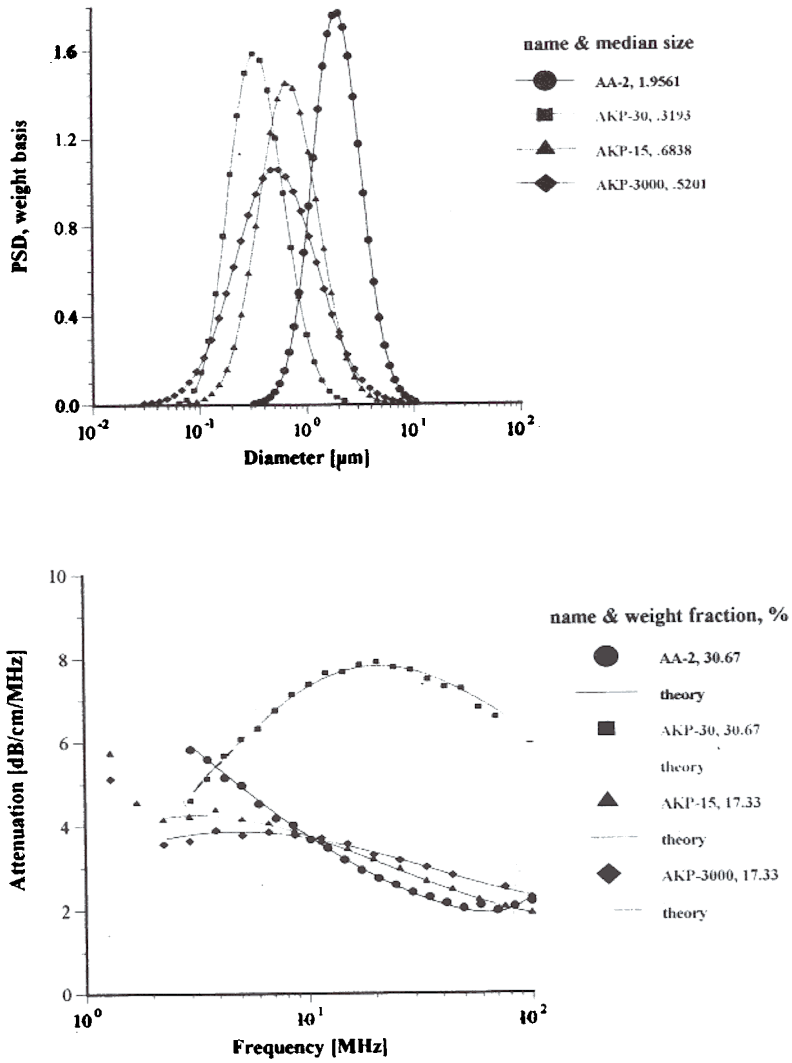

Fig. 4. Measured particle size distributions for four Sumitomo aluminas demonstrates the wide particle size range capability of acoustic spectroscopy and the ability to provide quality control of a wide range of raw materials. Acoustic Spectra for same four aluminas fit precisely with theoretical curve based on output particle size distribution.

a typical rutile and alumina sample using electroacoustic data. The pH at which the ζ-potential goes to zero is referred to as the isoelectric pH. Different materials may have quite different isoelectric points as is evident from this figure. If good stability is desired, then one needs to operate far enough from the isoelectric point to achieve a ζ-potential in excess of say 20–30 mV, either plus or minus. For the alumina shown this would suggest that to obtain optimum stability for this

Table 1
Median particle size of Aluminas Sumitomo

	Acoustics, DT-1200	Manufacturer
AKP-15	0.684	0.7
AKP-30	0.319	0.3
AKP-3000	0.520	0.5
AA-2	1.956	2

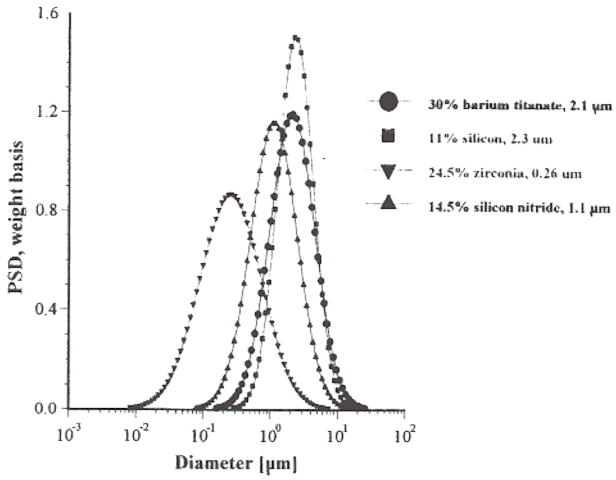

Fig. 5. Versatility of acoustic method is illustrated by particle size distributions for variety of ceramic materials.

alumina, one should adjust the pH to avoid the pH range between 8 and 11 where the ζ-potential is less than 20 mV. This complex relationship between ζ-potential and particle size distribution can be easily understood using acoustic spectroscopy [36].

In the real world, the situation is sometimes even more complex. The particle size and ζ-potential is not just a function of the final chemical state of the system, but may depend also on the history of how the system reached this state. In other words, the complete history of the sample may be important as is illustrated in Fig. 8, a case history of a plant manufacturing silicon nitride. The red curve shows the ζ-potential as the pH is decreased to an acid condition. From just this data alone one would think that a pH of 7–8 would provide adequate ζ-potential for stability. However, operating experience in the plant indicated otherwise. A clue to the problem was found by reversing the titration towards more alkaline conditions. The reverse titration, shown by the blue curve, revealed that the isoelectric point decreased by 2 pH units after the slurry was exposed to this acid condition. Investigation of plant operations showed that the slurry processing normally included such an acid wash. In order to obtain adequate stability following this acid condition, the data suggests that the process pH must be readjusted to a point either significantly below or above this new isoelectric point. But how can this dramatic shift in the isoelectric point be explained? The explanation is actually quite simple. The initial slurry had a very small level of contamination, which was insignificant in terms of the overall stability of the system. However, under acid conditions this minor component dissolved. Upon subsequent change to more alkaline conditions, this dissolved material re-precipitated on the surface of the major silicon nitride component. Now this minor component, although present only in seemingly insignificant quantity, nevertheless dominated the surface chemistry of the silicon nitride material. By realizing that the final state is dependent on the history of the sample the process could be modified to accommodate this change.

4.2. Chemical-polishing materials

Modern chemical-mechanical polishing materials (CMP) present a new challenge for measuring techniques. Three aspects of this application cause difficulties when using instruments based on traditional techniques. First, the particle size of a typical CMP slurry is too small for sedimentation based instruments or electric zone instruments. Typically, the mean size of CMP materials is approximately 100 nm with no particles, or hopefully just a few, larger than 500 nm. Second, the range in the size of the particles may be greater than 1000:1 which also eliminates many classical techniques. Third, CMP systems are typically shear sensitive. Shear caused by the polishing process itself or the delivery system may cause unpredictable assembly of the smaller particles into larger aggregates. However, these aggregates may be weakly formed and easily destroyed by subsequent sonication, high shear, or dilution. Therefore, any technique which requires dilution or other sample preparation steps may in fact destroy the very aggregates that one is attempting to quantify by measurement. It was suggested that CMP systems must be characterized as is, without any dilution or sample preparation.

Acoustic spectroscopy provides an exciting alternative to more classical methods. However,

there is one feature of acoustic spectroscopy which thus far has not been described sufficiently in the literature: namely the ability to characterize a bimodal PSD. Although Takeda et al. [39] demonstrated that acoustic spectroscopy is able to characterize bimodal distributions of mixed alumina particles, the ultimate sensitivity in detecting one very small sub-population in combination with another dominant mode has not yet been investigated. Yet, it is just this feature, the ability to recognize a small sub-population, which is most critical for CMP studies. The paper [40] addresses this important issue.

Unfortunately, there is no agreement in the literature as to the number of larger particles which might be allowed in a CMP slurry. For the

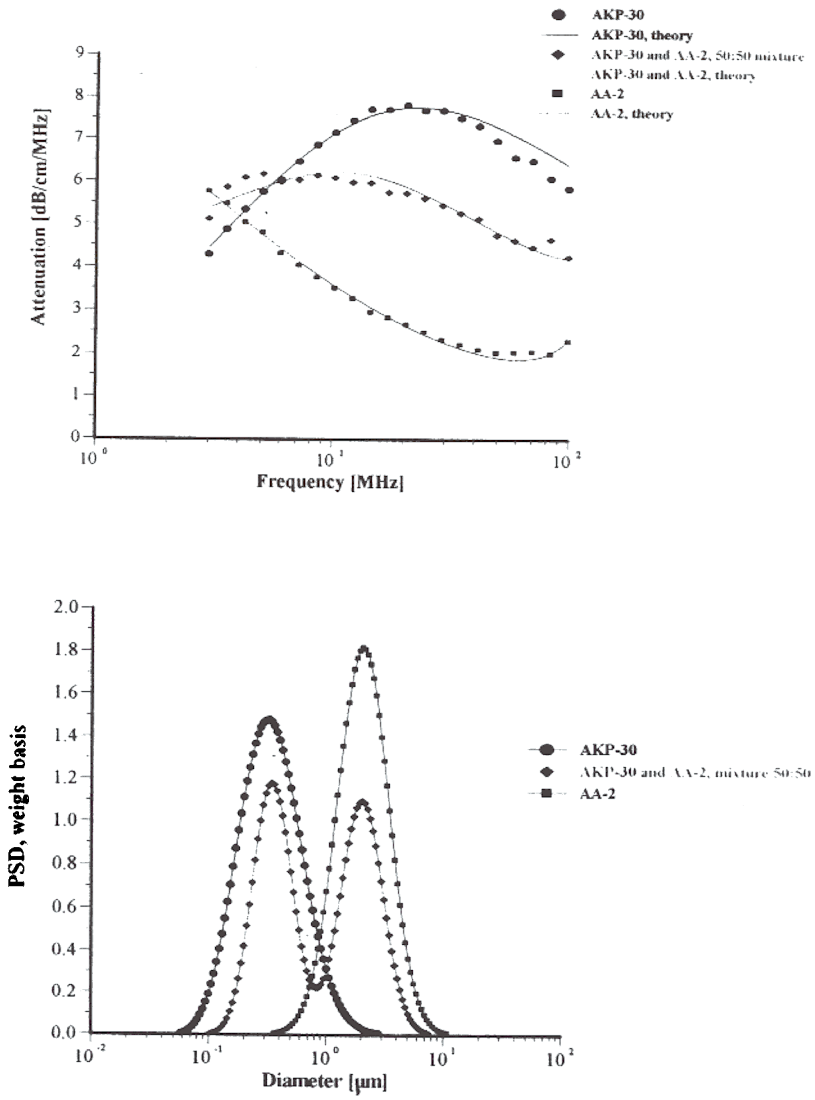

Fig. 6. The high sensitivity of acoustic attenuation spectra is illustrated by the large difference in the attenuation spectra for two different size alumina slurries as well as a 1:1 mixture of each. The validity of the theory is established by the good fit between the theoretical prediction and the experimental data. Each peak in the bimodal distribution for the mixed slurry agrees precisely with a corresponding peak in the size distribution for the single component slurry.

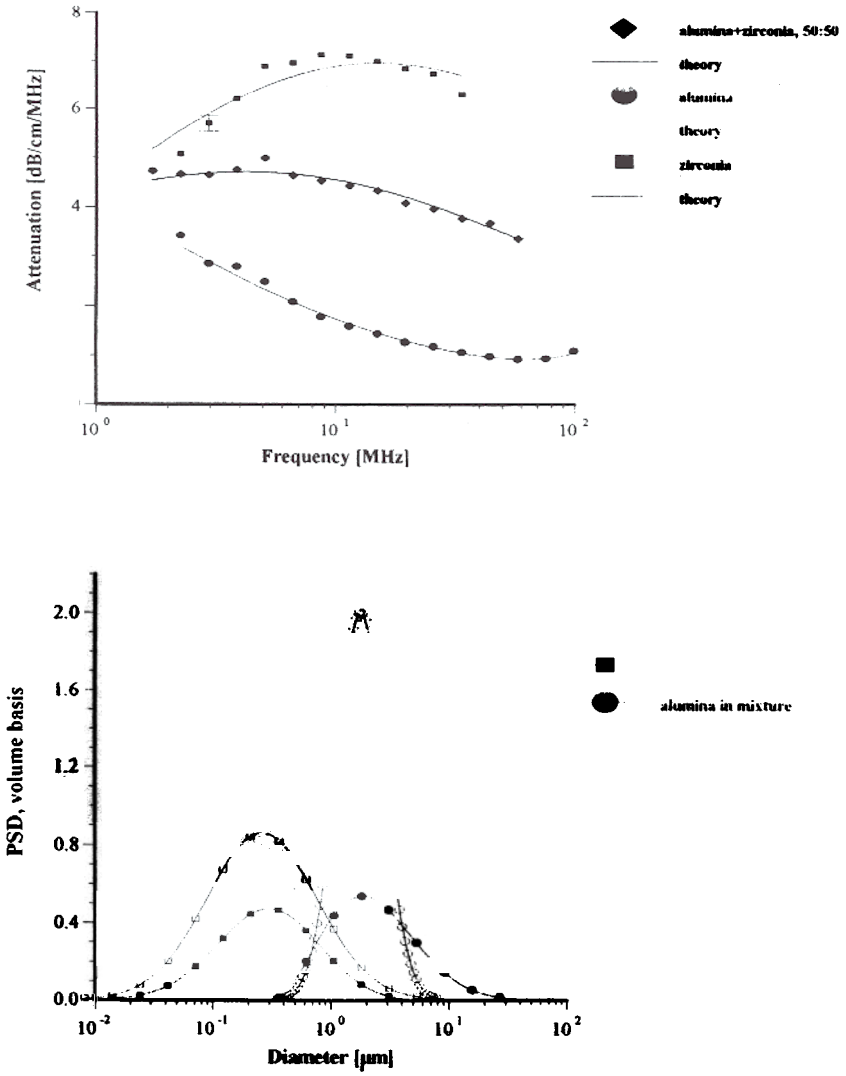

Fig. 7. The attenuation spectra for alumina, zirconia, and 1:1 mixture shows that three cases have quite different spectra and that best-fit theoretical distribution find good solution for each case. Particle size distribution for each component in mixed slurry can be measured. The size distribution for each component in the mixed slurry agrees well with the particle size for each component measured separately.

moment it will be assumed that only one large particle of 1 μm size might be allowed per 100 000 small 100 nm particles. This target sensitivity corresponds to large particles amounting to 1% of the total weight of all particulates.

Of course, an acoustic spectrometer does not directly measure particle size. In fact, it measures an attenuation spectra and calculates the particle size assuming a certain model for describing the sound attenuation in terms of the physical properties of the system. It follows therefore that this target sub-population sensitivity needs to be translated into a corresponding precision and accuracy specification for the attenuation measurement. It was shown in the paper [40] that, from a theoretical standpoint, the required precision is

roughly 0.01 dB cm^{-1} MHz^{-1}. The set of experiments were performed with a single component system of Dupont silica Ludox-TM to confirmed that DT-1200 acoustic spectrometer indeed meets this target requirement.

A second set of experiments was then made to test whether the attenuation spectra changed reproducibly when a small amount of the larger particles was added to a single component slurry of smaller particles. Two slurries were used for the small particles: Ludox-TM and Cabot SS25. Two Geltech silica with nominal sizes 0.5 and 1.5 μm were used as the model large particles. It was shown that the change in the attenuation spectra was statistically significant when the large particles amounted to at least 2% of the total weight of

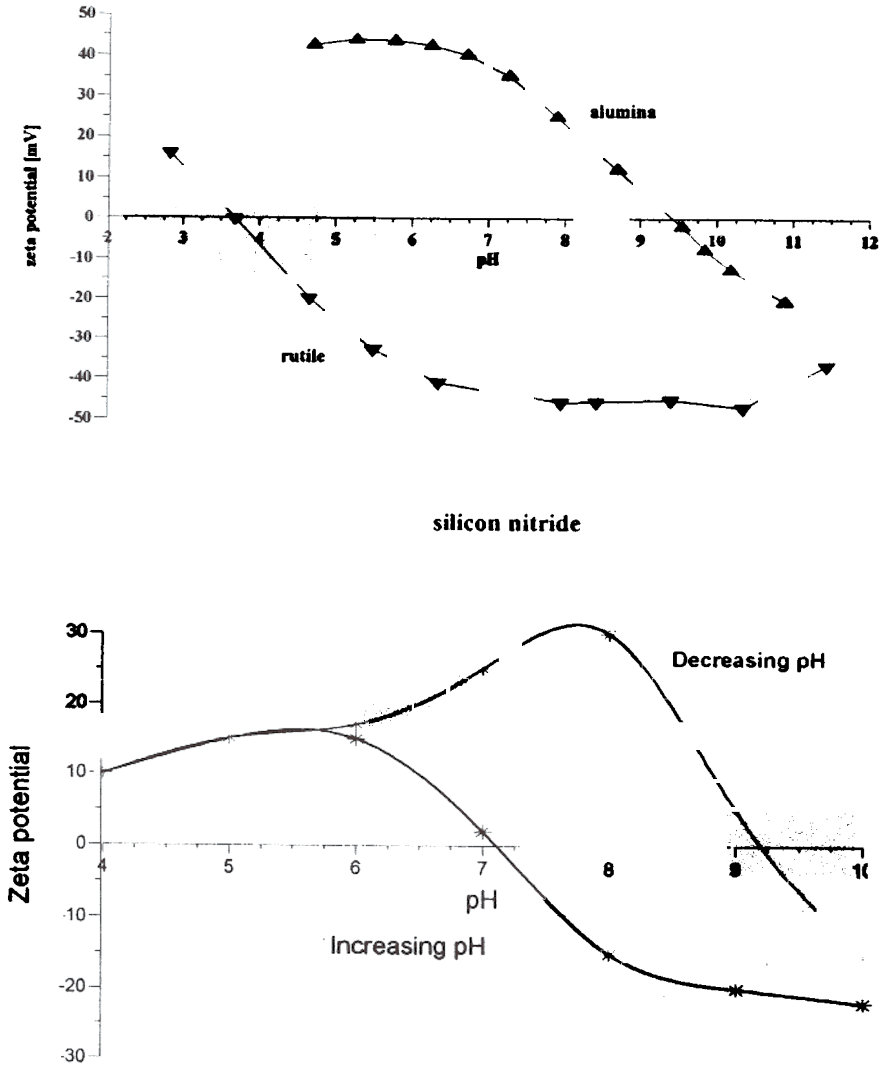

Fig. 8. Slurry isoelectric point suggests optimum pH for achieving stability. Curve for alumina slurry suggests avoiding the range pH 9–10, whereas titania curve suggests avoiding the range pH 3–4. Slurry stability depends not only on chemical state but how one reaches this state. Titration of production silicon nitride to low pH indicates high ζ-potential and good stability at pH 7–8. However, process engineers found that this pH did not provide good operating performance. Actual process included an acid wash of slurry. Back titration to alkaline conditions shows dramatic shift in isoelectric point requiring shift in plant operating conditions.

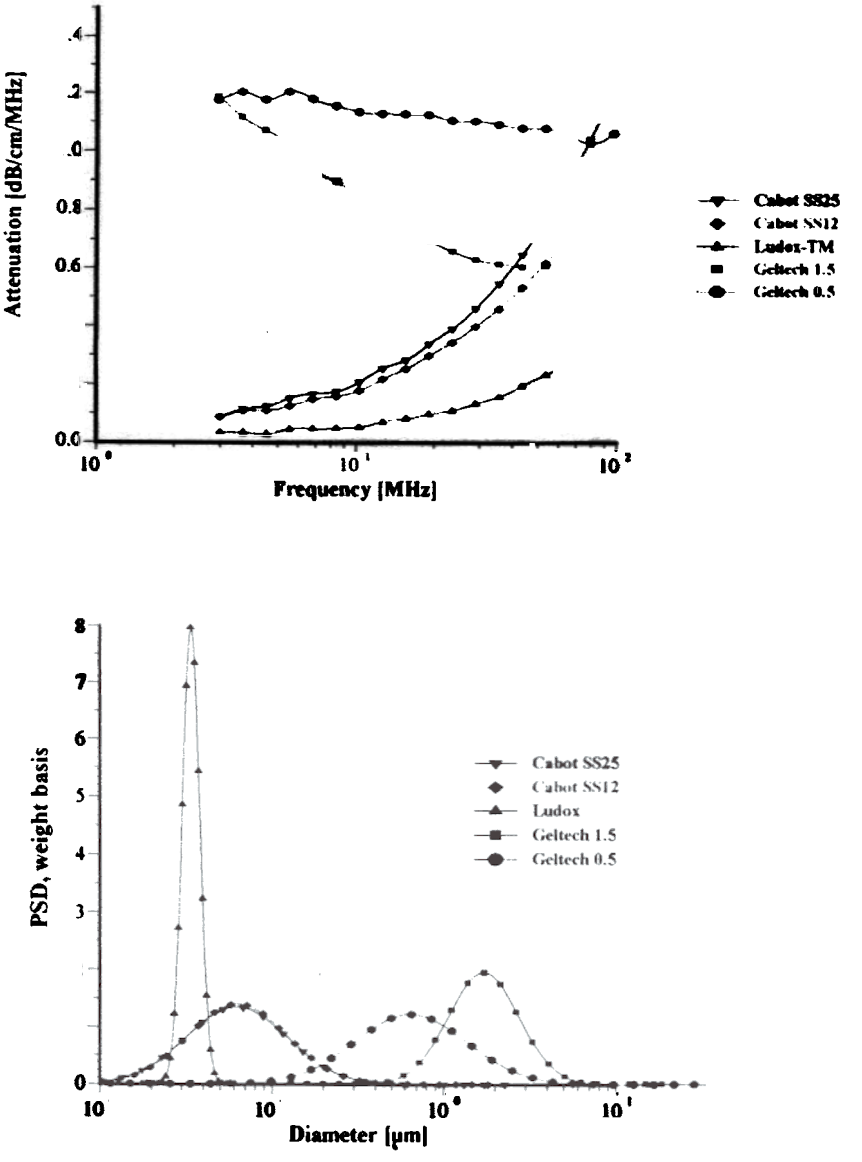

Fig. 9. Attenuation spectra measured for Ludox TM silica, Geltech 0.5 and 1.5 silica, Cabot SS25 and SS12silica. Total solid content is 12 wt.% except for SS25 which is 25 wt.%. Particle size distributions corresponding to the measured attenuation spectra.

all particulates. Expressed another way, the detection limit for this 12 wt.% slurry corresponded to a sub-population which was only 0.24 wt.% in terms of the total sample weight, or 0.24 g of large particles per 100 g of the slurry.

The attenuation spectra and corresponding PSD for all five single component silica slurries is shown in Fig. 9. These tests allowed one to compare the particle size determined by acoustic spectroscopy for the five 12 wt.% test slurries with independent data from the manufacturers. The values of the median size in each case is shown in Table 2. It is interesting to note that there is some difference between the acoustically measured data and that provided by the manufacturer. In large part this is related to differences in the characteri-

zation technique. For instance, the size of the Ludox-TM slurry is determined by Dupont using a titration method. This method yields an average size on an area basis. Acoustic spectroscopy gives a size on a weight basis, which for a polydisperse system will always be somewhat larger than an area based size. In addition acoustic spectroscopy implies some assumption about real dispersed system when particle size is being calculated from the attenuation spectra. Any measuring technique does the same. These assumptions and variation in physical properties which are involved into the calculation can cause some variation in size as well.

Successful reproducibility and reasonable agreement with other techniques then encouraged one to test the ability to correctly determine bimodal PSD. Ludox TM or CMP SS12 small particles were used as the major component of a slurry. The Geltech 0.5 or Geltech 1.5 were used as 'large' and 'larger' particles in the minor component of the mixed slurry. In each case the minor fraction was added to the Ludox-TM or the CMP SS12 systems in steps. Each addition increased the relative amount of the larger particles by 2%. The attenuation spectra was measured twice for each mixed system in order to demonstrate reproducibility.

Fig. 10 illustrate the results of these mixed system tests. It is seen that attenuation increases with increasing amounts of the 'large' or 'larger' particles. The increase in the attenuation with increasing doses of the Geltech content is in all cases significantly larger than precision of the instrument. This demonstrates that the DT-1200 data contains significant information about the small amount of large particles.

Table 2
Median particle size for various silica samples

	Manufacturer	Acoustics
Ludox™	22 nm (area basis)	30 nm (weight basis)
Geltech 0.5	0.5 μm	0.65 μm
Geltech 1.5	1.5 μm	1.72 μm
Cabot SS12		63 nm
Cabot SS25		62 nm

The final question is to determine whether the calculated PSD calculates a correct bimodal distribution for these mixed model systems. The DT-1200 always calculates a lognormal and a bimodal distribution which best fits the experimental data. These two PSD are best in the sense that the fitting error between the theoretical attenuation calculated for the best PSD and the experimental attenuation is minimized. These fitting errors are important criteria for deciding whether the lognormal or bimodal PSD is more appropriate for describing a particular sample. For instance, the PSD is judged to be bimodal only if the bimodal fit yields substantially smaller fitting error than a lognormal PSD. It was shown that fitting errors for the bimodal PSD is better than the lognormal for all of the mixed systems over the whole concentration range and for both the large and larger sized particles. According to the fitting errors, all PSD in the mixed systems are bimodal, which of course is correct for these known mixed systems.

Details about error analysis implemented into the DT instruments software are described in the papers [36,40].

Acoustics yields information only about particle size. It turned out that it is not sufficient for characterizing CMP slurries. Information about ζ-potential is very valuable for proper characterization of these materials. Electroacoustics opens the way to perform this characterization with very high quality of reproducibility and speed. Fig. 11 shows results of pH titration of silica Ludox and CMP slurry produced by ECC. It is seen that electroacoustics is able to characterize ζ-potential below 1 mV with precision about 0.1 mV. This degree of accuracy and precision exceeds anything imaginable with microelectrophoresis

4.3. Emulsions

There are many instances of successful characterization of the particle size distribution and ζ-potential of emulsion droplets. There are two quite representative reviews of these experiments published by McClements [3] (acoustics) and Hunter [8] (electroacoustics) (Fig. 12).

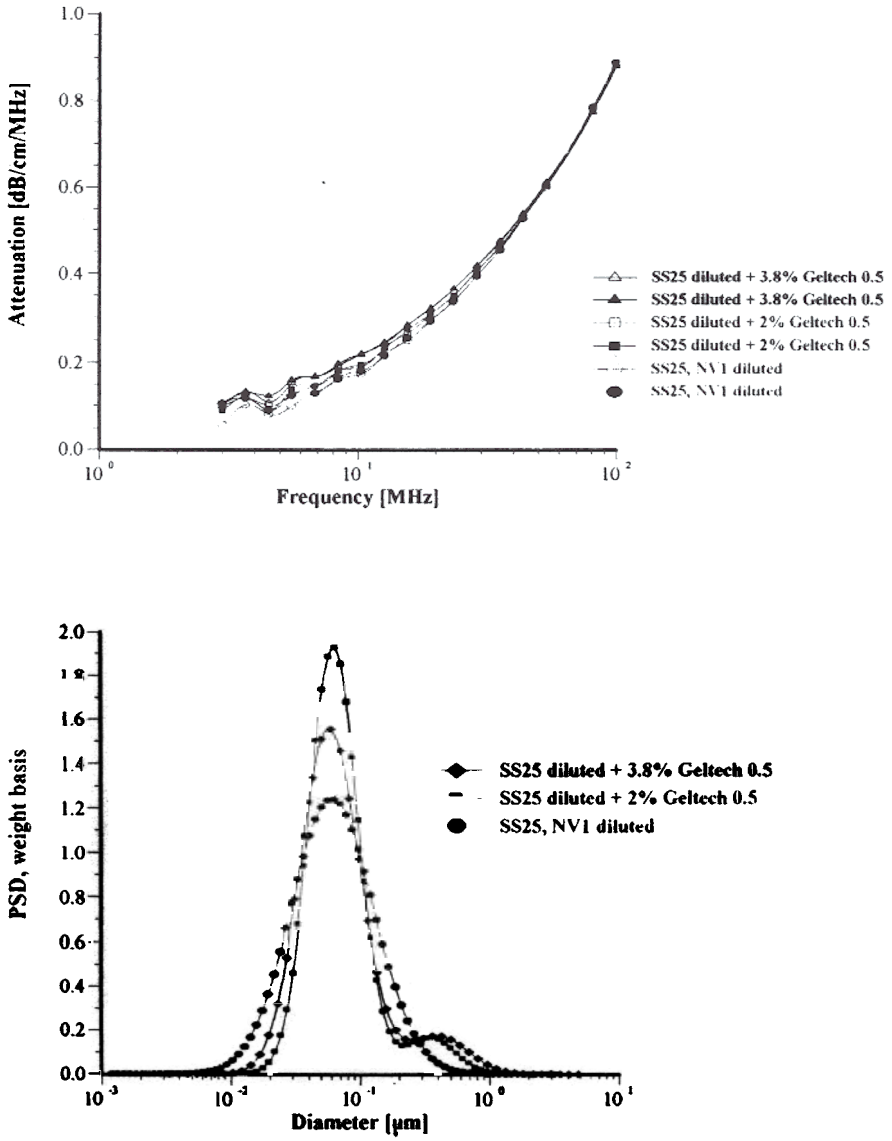

Fig. 10. Attenuation spectra and corresponding particle size distribution for Cabot SS25 silica diluted down to 12 wt.% with various additions of Geltech 0.5 silica. Total solid content is 12 wt.%. Legend shows the fraction of the total solid content corresponding to the silica Geltech.

Some results of a recent investigation are presented that were not published before. Various factors that affected stability, size and ζ-potential of the emulsion droplets were investigated.

One of the most important parameter affecting emulsions is the surfactant concentration that affects surface chemistry. This factor was tested for reverse water-in-oil emulsion. The oil phase was simply commercially available car lubricating oil diluted twice with paint thinner in order to reduce the viscosity of the final sample. Fig. 13 illustrates results for emulsions prepared with 6% by weight of water.

This Figure shows the attenuation spectra for three samples. The first sample was a pure oil phase and exhibited the lowest attenuation. It is important to measure the attenuation of the pure dispersion medium when a new liquid is evaluated. In this particular case, the intrinsic attenuation of the oil phase was almost 150 dB cm^{-1} at 100 MHz which is more than seven times higher than for water. This intrinsic attenuation is a very important contribution to the attenuation of ultrasound in emulsions. It is the background for characterizing emulsion system.

The emulsion without added surfactant was measured twice with two different sample loads. As the water content was increased the attenuation became greater in magnitude. For this system, the attenuation was found to be quite stable with time. Addition of 1% by weight sodium bis 2-ethylhexyl sulfosuccinate (AOT) changed the attenuation spectra dramatically. This new emulsion with modified surface chemistry was measured two times in order to show reproducibility. The corresponding particle size distribution is shown in Fig. 13 and indicates that the AOT converted the regular emulsion into a microemulsion as one could expect.

These experiments proved that the acoustic technique is capable of characterizing the particle size distribution of relatively stable emulsions. In many instances emulsions are found that are not stable at the dispersed volume concentration required to obtain sufficient attenuation signals (usually above 0.5%). Hazy water in fuel emulsions (diesel, jet fuel, gasoline) may exist at low water concentrations of only a few 100 ppmv (0.01%) of dispersed water. Attempts at characterizing these systems without added surfactant resulted in unstable attenuation spectra and water droplets were discovered to separate from the bulk emulsion and settle out on the chamber walls. This problem is less important for thermodynamically stable microemulsions.

4.4. Food emulsions

Food emulsions is a very important and prospective application for acoustics and electroacoustics. These emulsions are quite concentrated which eliminates traditional light based techniques for characterization purposes. Dilution protocol is not suitable for emulsions because it destroys the original distribution of droplets.

Fig. 14 illustrate that acoustic spectrometer is able to provide reproducible and distinguishable attenuation spectra for a wide spectrum of dairy products. One can see that attenuation spectra

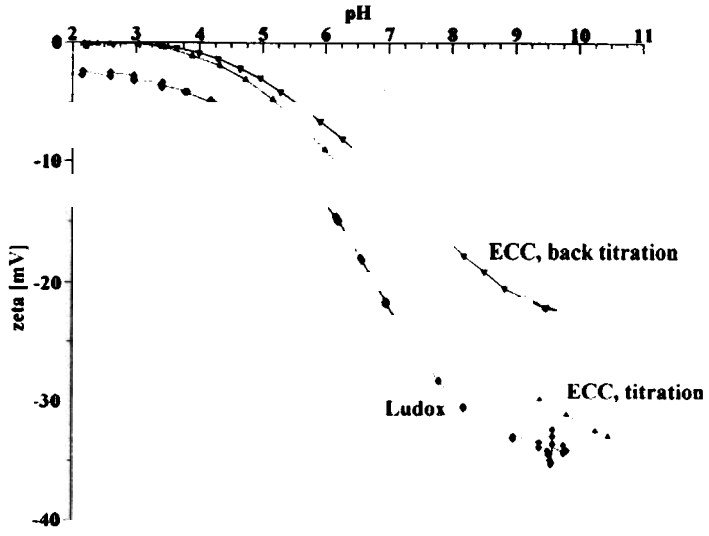

Fig. 11. Titration of silica Ludox TM at 10 wt.% and chemical-mechanical polishing silica ECC

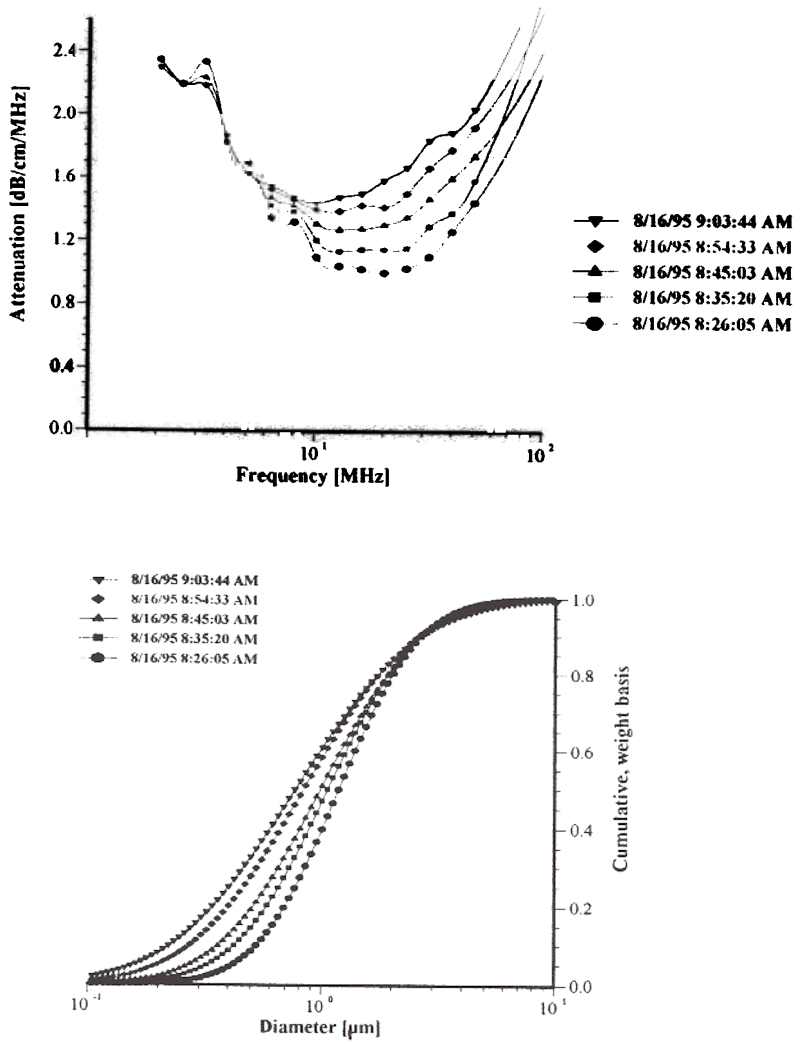

Fig. 12. Attenuation spectra and droplet size distribution of 40% water in cyclo methicone emulsion.

reflects a fat content. There is a general trend of increasing attenuation with increasing fat content.

Attenuation spectra contains information about droplets size. This PSD can be calculated using certain input parameters. In the case of emulsions sound speed, thermal expansion and intrinsic attenuation of the fat oil need to be known. In principle these parameters are easily measurable if one has fat oil as a one phase liquid. Unfortunately, dairy fat oil is not available at least here as a pure liquid.

Nevertheless, other oils with close properties can be used. In this particular case sound speed was assumed equal to 1440 m s^{-1}, thermal expansion to 7.2×10^{-4} 1 K^{-1}, intrinsic attenuation to 5 dB cm $^{-1}$ MHz^{-1} at 100 MHz which is 25 times higher than water. Content of fat is 25 wt.% for ranch and 17 wt.% for maonese. Droplets size distribution for ranch salad dressing and mayonese corresponding to these input parameters are given on Fig. 14.

It is important to mention that different input parameters would lead to the different droplet size distributions. However, even this PSD are somewhat helpful for understanding difference between size of the different dairy products. It can be used for this purpose especially keeping in mind high reproducibility illustrated on Fig. 15.

4.5. Microemulsions

The mixture of heptane with water and AOT is a classic three component system. It has been widely studied due to a number of interesting features it exhibits. This system forms stable reverse microemulsions (water in oil) without the complication introduced by additional co-surfactant. Such a co-surfactant (usually alcohol) is required by many other reverse microemulsion systems. This simplification makes the alkane/water/AOT system a model for studying reverse microemulsions.

There have been many studies devoted to characterization of these practically important systems. Reverse emulsion droplets have been used as chemical micro reactors to produce nano size inorganic and polymer particles with special properties that are not found in the bulk form [41–45]. These microemulsion systems have also been a

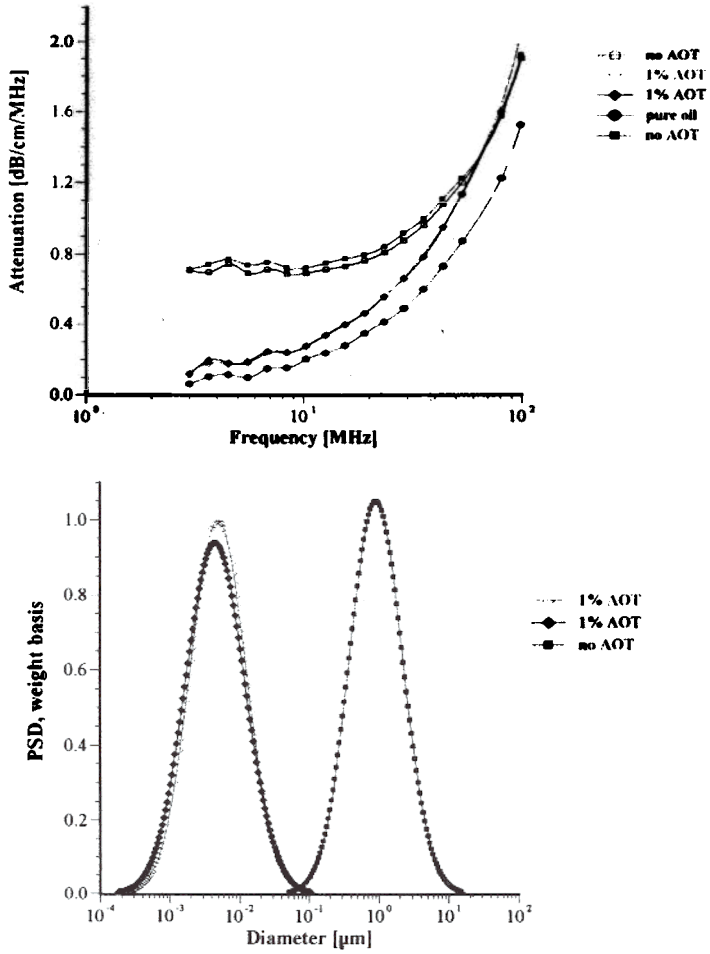

Fig. 13. Attenuation and corresponding particle size distribution of 6 wt.% water-in-car oil emulsion and microemulsion created by adding sodium bis 2-ethylhexyl sulfosuccinate (AOT).

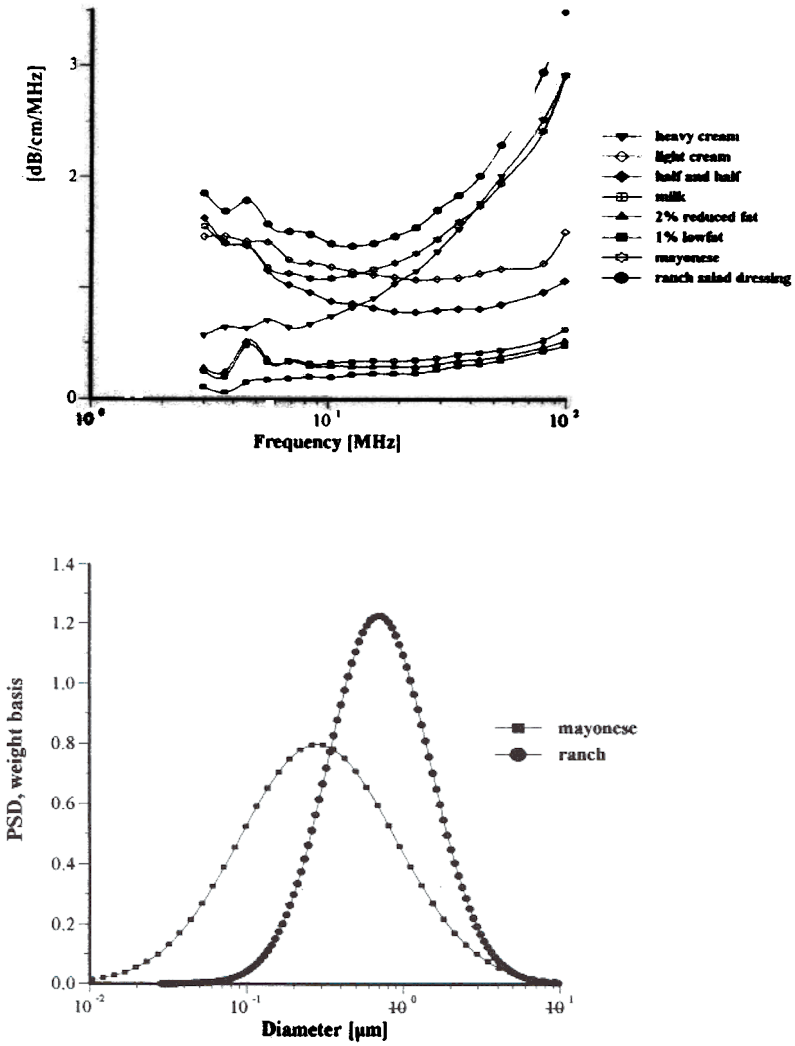

Fig. 14. Attenuation spectra of the various dairy products and corresponding PSD.

topic of research for biological systems and the AOT head groups have been found to influence the conformation of proteins and increase enzyme activity [46–49]. The unique environment created in the small water pools of swollen reverse micelles allows for increased chemical reactivity. The increase in surface area with decrease in size of the droplets also can significantly increase reactivity by allowing greater contact of immiscible reactants.

There have been many attempts to measure the droplet size of this microemulsion. Several different techniques were used: PCS [50–55], classic light scattering [52,54,56], SANS [57–59], SAXS [51,60,61], ultracentrifugation [49,53,56], and viscosity [51,53,56]. It was observed that the heptane/water/AOT microemulsions have water pools with diameters ranging from 2 up to 30 nm. The water drops are encapsulated by the AOT surfactant so that virtually all of the AOT is located at the interface shell. The size of the water droplets can be conveniently altered by adjusting the molar ratios of water to surfactant designated as R ($[H_2O]/[AOT]$). At low R values ($R < 10$) the wa-

ter is strongly bound to the AOT surfactant polar head groups and exhibits unique characteristics different from bulk water [56]. At higher water ratios, ($R > 20$), free water is predominant in the swollen reverse micellular solutions, and at approximately $R = 60$, the system undergoes a transition from a transparent microemulsion into an unstable turbid macroemulsion. This macroemulsion separates on standing into a clear upper phase and a turbid lower phase.

The increase in droplet size and phase boundary can also be achieved by raising the temperature up to a critical temperature of 55°C. In addition this system has been found to exhibit an electrical percolation threshold whereby the conductivity increases by several orders of magnitude by either varying the R ratio or increasing the temperature [59,60,62,63]. Despite all these efforts, there still remain questions regarding the polydispersity of the water droplets, and few studies are available above the R value of 60 where a turbid macroemulsion state exists.

Acoustic spectroscopy offers a new opportunity for characterizing these complicated systems. Details of this experiment are presented in the paper [64]. The reverse microemulsions were prepared by first making a 0.1 molar AOT in heptane solution (6.1 wt.% AOT). The heptane was obtained from Sigma as HPLC grade (99 + % purity). Known amounts of 18 MΩ-cm water were added to the AOT-heptane solution using a 1 ml total volume, graduated glass syringe and then shaken for 30 s in Teflon capped glass bottles. The shaking action was required to overcome an energy barrier to distribute the water into the nano-sized droplets, as it could not be achieved using a magnetic stirrer.

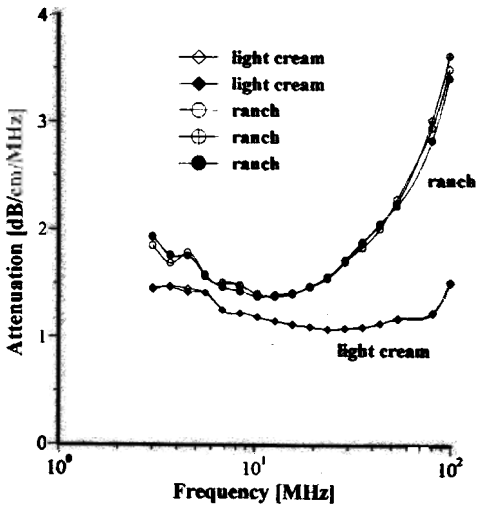

Fig. 15. Attenuation spectra of ranch salad dressing and light cream measured several times for illustrating reproducibility.

In all cases, the reported R values are based on the added water, and were not corrected for any residual water that may have been in the dried AOT or heptane solvent. Karl Fischer analysis of the AOT-heptane solutions before the addition of water resulted in an R value of 0.4. This amount was considered to be negligible.

Measurements were made starting with the pure water and heptane and then the AOT-heptane sample with no added water ($R = 0$). The sample fluid was removed from the instrument cell and placed in a glass bottle with a Teflon cap. Additional water was titrated and the microemulsion was shaken for 30 s before being placed back into the instrument cell. The sample cell contained a cover to prevent evaporation of the solvents. The samples were visually inspected for clarity and rheological properties for each R value. These steps were repeated for increasing water weight fraction or R ratios up to $R = 100$. At $R \geq 60$ the microemulsions became turbid. At $R > 80$, the emulsions became distinctly more viscous.

The weight fractions of the dispersed phase were calculated for water only without including the AOT. Each trial run lasted approximately 5–10 min with the temperature varied from 25 to 27°C. A separate microemulsion sample for $R = 40$ was made up a few days prior to the first study. For the $R = 70$ sample, a second acoustic measurement was made with the same sample used for the first study. The complete set of experiments for water, heptane, and the reverse microemulsions from $R = 0–100$ was repeated to evaluate the reproducibility.

Attenuation spectra measured in the first run up to $R = 80$ are presented in Fig. 16. The results for $R = 90$ and $R = 100$ are not reported because they were found to vary appreciably. As the water concentration is increased, the attenuation spec-

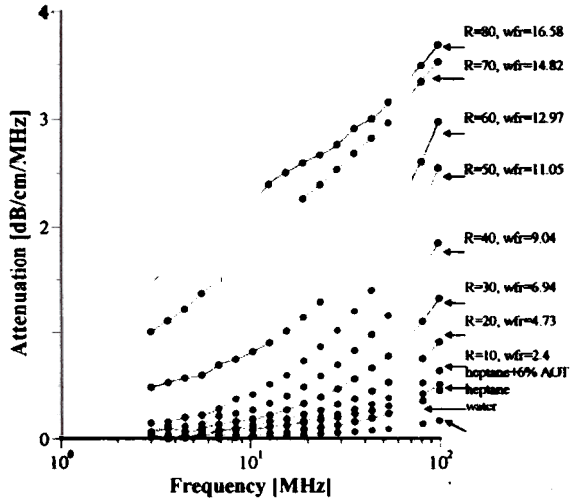

Fig. 16. Acoustic attenuation spectra measured for water/sodium bis 2-ethylhexyl sulfosuccinate (AOT)/heptane system for different water to AOT ratios R.

trum rises in intensity and there is a distinct jump in the attenuation spectrum from $R = 50$ to $R = 60$ in the low frequency range. This discontinuity is also reflected in the visual appearance as at $R = 60$ the system becomes turbid. The smooth shape of the attenuation curve also changes at $R > 60$. The stability and reproducibility of the system was questioned due to the irregular nature of the curve so the experiment at $R = 70$ was repeated and gave almost identical results. An additional experiment was run at $R = 40$ for a separate microemulsion prepared a few days earlier. This showed excellent agreement with the results for freshly titrated microemulsion.

For R values > 70, an increase in the viscosity and a decrease in the reproducibility of the attenuation measurement were observed. This could be due to the failure of the model for this system as a collection of separate droplets at high R values.

The two lowest attenuation curves correspond to the attenuation in the two pure liquids; water and heptane. This attenuation is associated with oscillation of liquid molecules in the sound field. If these two liquids are soluble in each other, the total attenuation of the mixture would lie between these two lowest attenuation curves. But it can be seen that the attenuation of the mixture is much higher than that of the pure liquids. The increase in attenuation, therefore, is due to this heterogeneity of the water in the heptane system. The extra attenuation is caused by motion of droplets, not separate molecules. The scale factor (size of droplets) corresponding to this attenuation is much higher than that for pure liquids (size of molecules).

The current system contains a third component-AOT. A question arises on the contribution of AOT to the measured attenuation. In order to answer this question, measurements were done on a mixture of 6.1 wt.% AOT in heptane ($R = 0$). It is the third smallest attenuation curve on Fig. 13. It is seen that attenuation increases somewhat due to AOT. However, this increase is less than the extra attenuation produced by water droplets. The small increase in attenuation is attributed to AOT micelles. Unfortunately thermal properties of the AOT as a liquid phase are not known and the size of these micelles could not be calculated.

The particle size distributions corresponding to the measured attenuation spectra are presented in Fig. 15. It can be seen that the distribution becomes bimodal for $R \geq 60$ that coincides with the onset of turbidity. It is to be noted that such a conclusion could not easily be arrived at with other techniques. However, Fig. 17 illustrates a peculiarity of this system that can be compared with independent data from literature: mean particle size increases with R almost in a linear fashion. This dependence becomes apparent when mean size is plotted as a function of R as in Fig. 18.

It is seen that mean particle size measured using acoustic spectroscopy are in good agreement with those obtained independently using the neutron scattering (SANS) and X-ray scattering (SAXS) techniques [46,51,57] for R values ranging from 20 to 60. A simple theory based on equi-partition of water and surfactant [36] can reasonably explain the observed linear dependence.

At $R = 10$ the acoustic method gave a slightly larger diameter than expected. This could be due to the constrained state of the 'bound water' in the swollen reverse micelles. The water under these conditions may exhibit different thermal properties than the bulk water used in the particle

size calculations. Also at the low R values ($R < 10$ or $< 2.4\%$ water), the attenuation spectrum is not very large as compared to the background heptane signal. Contribution of droplets to attenuation spectrum then may become too low to be reliably distinguished from the background signal coming from heptane molecules and AOT micelles.

In addition to particle size, the Colloid Vibration Current was also measured for calculating ζ-potential. The results are presented in Fig. 19 and the ζ-potential was found to depend on the water content. An increased concentration of water resulted in higher ζ-potentials. However, the water content was not the most important factor. This experiment was performed at two different AOT concentrations and the ratio of water to AOT (R) was discovered to be the key parameter. When the ζ-potential was plotted versus the R values, the same curve was obtained for both AOT concentrations. This demonstrates that the ζ-potential depends on the degree of the water surface coverage by AOT molecules.

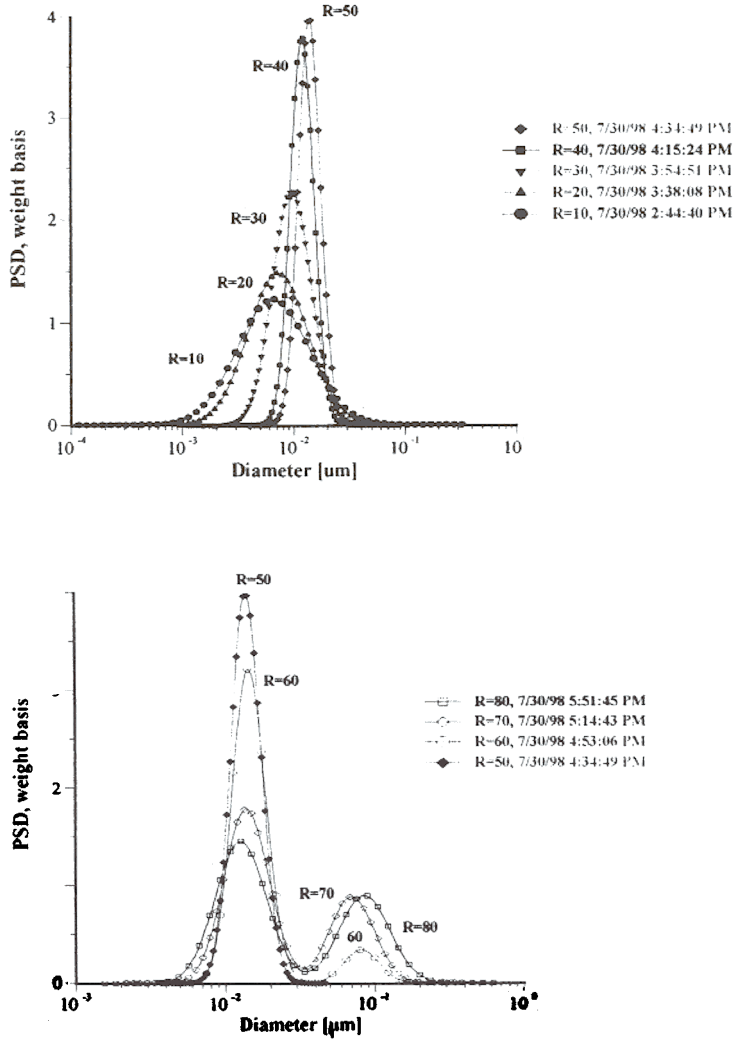

Fig. 17. Drop size distribution for varying R [H_2O]/[sodium bis 2-ethylhexyl sulfosuccinate (AOT)] from 10 to 50 and from 50 to 80.

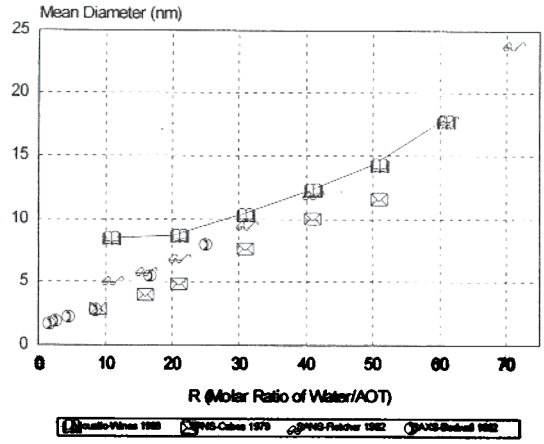

Fig. 18. Comparison of mean droplet size measured using acoustic spectroscopy, neutron scattering and X-ray scattering.

This experiment allows one to suggest a mechanism of electric charge formation on the surface of the water droplets in the oil phase. This is a field of great interest in modern emulsion science. According to the experiment, the ζ-potential appears when there is a deficit of AOT molecules for complete coverage of the water droplets. As more elements of the water phase become exposed to the oil, higher values of the ζ-potential are measured. The water phase also contains a considerable concentration of sodium ions that originate from the AOT and serve as counter-ions to the negatively charged sulfosuccinate head groups. As a result of decreased surface coverage, the water droplets gain surface charge when they are in contact with oil. This surface charge can appear because of ion exchange between the water and oil phase caused by the difference in standard chemical potentials in each phase. Molecules of AOT do not create surface charge, but conversely screen the surface charge of the initial water droplets. At the same time these AOT molecules change the interfacial tension creating conditions for a thermodynamically stable microemulsion. This is only a hypothesis so far and further investigation is required for confirmation.

4.6. Latex

There have been many successful experiments that have characterized latex systems using both acoustics and electroacoustics. For instance, Allegra and Hawley measured polystyrene latex. There is another successful application, this time with neoprene latex, which is described in the paper [15].

The accuracy and precision of the D-1200 Acoustic Spectrometer have also been tested using Standard Dow Latex with expected median particle size of 0.083 μm. Results are shown in the Table 3.

These successful examples of characterizing latex systems are possible only when thermal expansion coefficients are known. Unfortunately, this parameter is not known for many latex polymers. This problem becomes even more complicated for latex systems than for emulsions because the value of the thermal expansion depends strongly on the chemical composition of the polymer. Fig. 20 illustrates this fact for several ethylene copolymers with different ethylene content. Variation of the ethylene content from 5 to 10% was found to causes significant change in attenuation spectra. This change is associated with the thermal expansion coefficient, but not the particle size.

The uncertainty related with the thermal expansion coefficient makes latex systems the most complicated systems for acoustics. This is important to keep in mind for testing a particular model of an acoustic instrument. Latex dispersions that are used as standards for light based methods should be used with caution as in many cases the thermal expansion properties of these standards are not well known.

5. Conclusions

It is hoped that it is proven with this short review that acoustics and electroacoustics can be extremely helpful in characterizing particle size, ζ-potential and some other properties of concentrated dispersed systems. Both methods are commercially available already. There are still some problems with theoretical background for elec-

troacoustics of emulsions but analysis of the literature shows gradual improvement in this field.

The combination of the acoustic and electroacoustic spectroscopy provides a much more reliable and complete characterization of the disperse system than either one of those spectroscopes separately. Electroacoustic phenomena is more complicated to be interpreted when comparing the acoustic ones because an additional field (electric) is involved. This problem becomes even more pronounced for a concentrated system. It makes acoustics favorable for characterizing particle size,

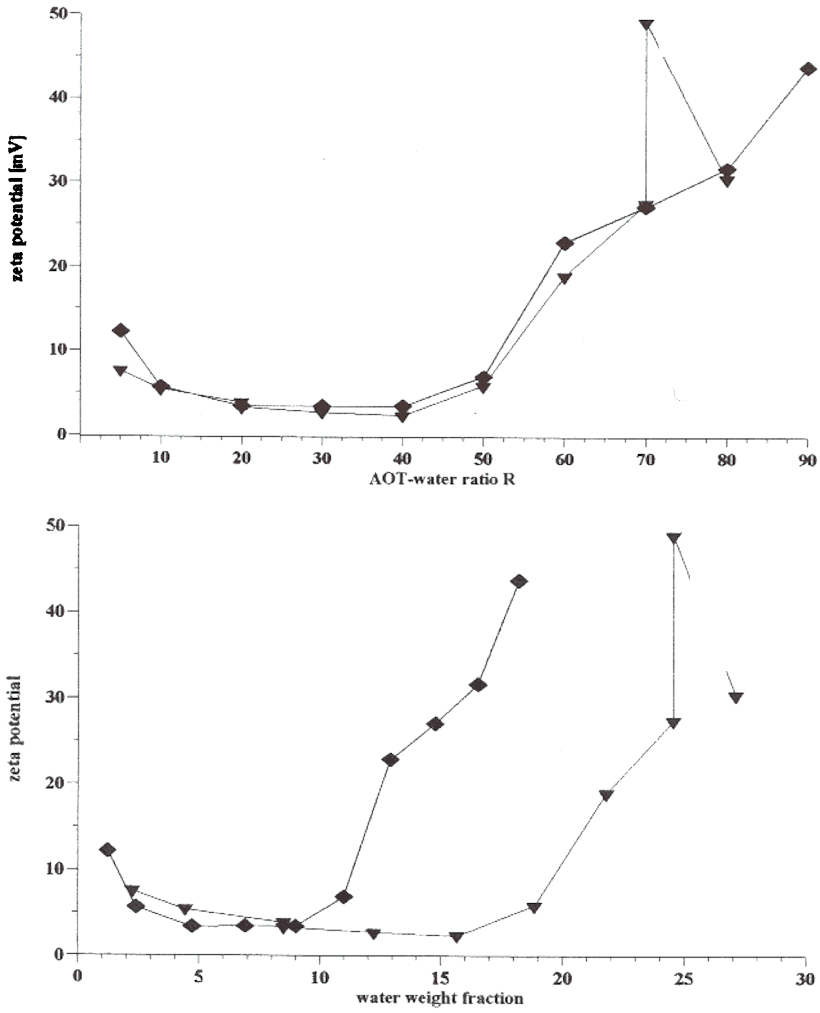

Fig. 19. ζ-Potential measured electroacoustically for water droplets covered with sodium bis 2-ethylhexyl sulfosuccinate (AOT) in heptane vs. water content.

Table 3
Median diameter measured for 10 wt.% latex Serva 44405, Standard Dow latex with expected median size of 0.083 μm

# Meas.	1	2	3	4	5	6	7	8	9	10
Median diameter (μm)	0.0767	0.0765	0.0867	0.0823	0.0775	0.0737	0.0713	0.081	0.076	0.0754

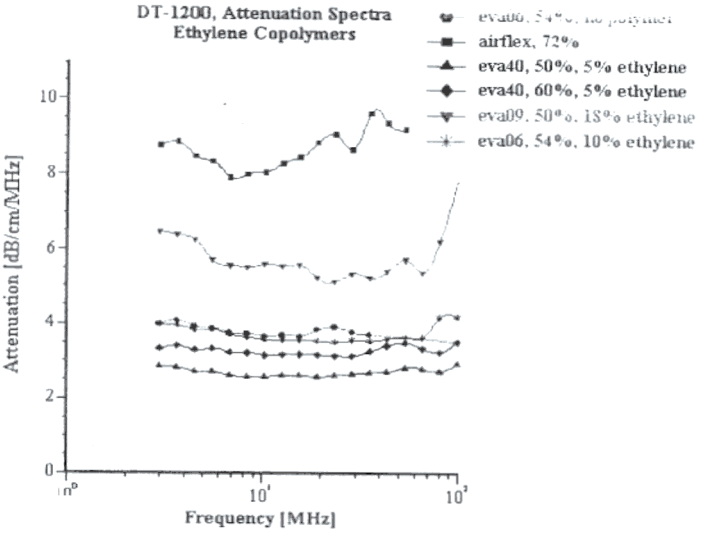

Fig. 20. Attenuation spectra for latex dispersions with different content of ethylene.

whereas electroacoustics yields electric surface properties.

It is believed that these ultrasound based techniques is a very valuable addition to the traditional colloid chemical arsenal of tools designed for characterizing surface phenomena.

Appendix A

According to the paper [18] drag coefficient can be expressed in the following form general for both Kuvabara and Happel cell models:

$$\Omega = -\frac{\alpha^2}{3}\left(\frac{d(C_1h_1 + C_2h_2}{dx} + \frac{C_1h_1 + C_2h_2}{\alpha}\right) - \frac{4j\alpha^2}{9} \qquad \text{(A1)}$$

where x is normalized same way as α, coefficients C_1 and C_2 are different for two cell models:

	Kuvabara	Happel
C_1	$\frac{h_2(b)}{I}$	$\frac{bh_2(b)-2I_{23}}{bI+2(I_2I_{13}-I_1I_{23})}$
C_2	$\frac{h_1(b)}{I}$	$\frac{bh_1(b)-2I_{13}}{bI+2(I_2I_{13}-I_1I_{23})}$

where b is radius of the cell:

$$b^3 = \frac{a^3}{\varphi}$$

There are several special functions used in this theory. They are specified below.

$$H(\alpha) = \frac{ih(\alpha)}{2\alpha} - \frac{idh(x)}{2dx}$$

$$h(x) = h_1(x)h_2(\beta) - h_1(\beta)h_2(x)$$

$$I = I(\beta) - I(\alpha)$$

$$I(x) = -h_1(\beta) \times e^{x(1+j)}\left[\frac{3(1}{2\beta^3} + j\left(\frac{x^2}{\beta^3} - \frac{3x}{2\beta^3}\right)x\right] + h_2(\beta) \times e^{-x(1+j)}\left[\frac{3(1+x)}{2\beta^3} + j\left(\frac{x^2}{\beta^3} + \frac{3x}{2\beta^3}\right)\right.$$

$$I_1 = -j\frac{e^{-x(1+j)}}{x}\Big|_{x=a}^{x=b}$$

$$I_2 = -j\frac{e^{x(1+j)}}{x}\Big|_{x=a}^{x=b}$$

$$I_{13} = -\frac{e^{-x(1+j)}}{b^3}[1.5(x+1)+j(x^2+1.5x)]_{x=a}^{x=b}$$

$$I_{23} = \frac{e^{x(1+j)}}{b^3}[1.5(x-1)+j(-x^2+1.5x)]_{x=a}^{x=b}$$

$h_1(x)$

$$\frac{\exp(-x)}{\quad}\left[\frac{x+}{\quad}\right.$$

$$\left.+j\left(\frac{x+1}{x}\cos x+\sin x\right)\right]$$

$h_2(x)$

$$\frac{\exp(x)}{x}\left[\frac{x-}{x}\sin x+\cos x\right.$$

$$\left.+j\left(\frac{1-x}{x}\cos x+\sin x\right)\right]$$

Cell model in Happel version is more suitable for acoustics because it reflects properly hydrodynamic dissipation within the cell. Cell model in Kuvabara version is better for electroacoustics because it automatically yields Onsager relationship [30].

References

[1] J.R. Pellam, J.K. Galt, J. Chem. Phys. 14 (10) (1946) 608–613.
[2] C.T.J. Sewell, Phil. Trans. R. Soc. Lond. 210 (1910) 239–270.
[3] P.S. Epstein, R.R. Carhart, J. Acoust. Soc. Am. 25 (3) (1953) 553–565.
[4] D.J. McClements, Adv. Colloid Interface Sci. 37 (1991) 33–72.
[5] V.A. Hackley, J. Texter (Eds.), Ultrasonic and Dielectric Characterization Techniques for Suspended Particultes, The American Chemical Society, Ohio, 1998.
[6] J. Lyklema, Fundamentals of Interface and Colloid Science, vol. 1, Academic Press, New York, 1993.
[7] R.J. Hunter, Foundations of Collid Science, Oxford University Press, Oxford, 1989.
[8] R.J. Hunter, Colloids Surf. 141 (1998) 37–65.
[9] T.A. Strout, Attenuation of Sound in High-Concentration Suspensions:Development and Application of an Oscillatory Cell Model, A Thesis, The University of Maine, 1991.
[10] J.R. Allegra, S.A. Hawley, J. Acoust. Soc. Am. 51 (1972) 1545–1564.
[11] J.D. McClements, Colloids Surf. 90 (1994) 25–35.
[12] D.J. McClements, J. Acoust. Soc. Am. 91 (2) (1992) 849–854.
[13] A.K. Holmes, R.E. Challis, D.J. Wedlock, J. Colloid Interface Sci. 156 (1993) 261–269.
[14] A.K. Holmes, R.E. Challis, D.J. Wedlock, J. Colloid Interface Sci. 168 (1994) 339–348.
[15] A.S. Dukhin, P.J. Goetz, C.W. Hamlet, Langmuir 12 (21) (1996) 4998–5004.
[16] L.W. Anson, R.C. Chivers, Ultrasonic 28 (1990) 16–25.
[17] N.L. Catton, The Neoprenes, Rubber Chemical Division, E.I. Du Pont De Nemours, Wilmington, DW, 1953.
[18] A.S. Dukhin, P.J. Goetz, Langmuir 12 (21) (1996) 4987–4997.
[19] A.H. Harker, J.A.G. Temple, J. Phys. D.: Appl. Phys. 21 (1988) 1576–1588.
[20] R.L. Gibson, M.N. Toksoz, J. Acoust. Soc. Am. 85 (1989) 1925–1934.
[21] U. Riebel, et al., Part. Part. Syst. Charact. 6 (1989) 135–143.
[22] A.S. Dukhin, H. Ohshima, V.N. Shilov, P.J. Goetz, Electroacoustics for concentrated dispersions, Langmuir 15, 10 (1999) 3445–3451.
[23] A.S. Dukhin, V.N. Shilov, H. Ohshima, P.J. Goetz, Electroacoustics phenomena in concentrated dispersions. New theory and CVI experiment, Langmuir 15, 20 (1999) 6692–6706.
[24] P.S. Waterman, R.J. Truell, Math. Phys. 2 (1961) 512.
[25] R. Chanamai, J.N. Coupland, D.J. McClements, Colloids Surf. 139 (1998) 241–250.
[26] S. Temkin, Phys. Fluids 4 (11) (1992) 2399–2409.
[27] S. Temkin, J. Acoust. Soc. Am. 103 (2) (1998) 838–849.
[28] R.W. O'Brien, J. Fluid Mech. 190 (1988) 71–86.
[29] R.W. O'Brien, Determination of Particle Size and Electric Charge, US Patent 5,059,909, Oct. 22 (1991).
[30] A.S. Dukhin, V.N. Shilov, Yu. Borkovskaya, Dynamic electrophoretic mobility in concentrated dispersed systems. Cell model. Langmuir 15, 10 (1999) 3452–3457.
[31] H. Ohshima, A.S. Dukhin, J.Colloid Interface Sci. 212 (1999) 449–452.
[32] L.L. Foldy, Propagation of sound through a liquid containing bubbles, OSRD Report No. 6.1–sr1130–1378, 1944.
[33] E.L. Carnstein, L.L. Foldy, J. Acoust. Soc. Am. 19 (3) (1947) 481–499.
[34] F.E. Fox, S.R. Curley, G.S. Larson, J. Acoust. Soc. Am. 27 (3) (1957) 534–539.
[35] S. Ljunggren, J.C. Eriksson, Colloids Surf. 129–130 (1997) 151–155.
[36] A.S. Dukhin, P.J. Goetz, Colloids Surf. 144 (1998) 49–58.
[37] A.S. Dukhin, P.J. Goetz, Method and device for characterizing particle size distribution and zeta potential in concentrated system by means of acoustic and electroacoustic spectroscopy, patent USA, pending.

[38] A.S. Dukhin, P.J. Goetz, Method and device for determining particle size distribution and zeta potential in concentrated dispersions, patent USA, pending.
[39] Shin-ichi Takeda, Characterization of ceramic slurries by ultrasonic attenuation spectroscopy, In: V.A. Hackley, J. Texter (Eds.), Ultrasonic and Dielectric Characterization Techniques for Suspended Particulates, American Ceramic Society, Westerville, OH, 1998.
[40] A.S. Dukhin, P.J. Goetz, Characterization of chemical polishing materials (monomodal and bimodal) by means of acoustic spectroscopy, Colloids and Surfaces 158 (1999) 343–354.
[41] J.P. Wilcoxon, R.L. Williamson, in: C.R. Safinya, S.A. Safran, P.A. Pincus (Eds.), Material Research Society Symposium Proc., Macromolecular Liquids, vol. 177, Materials Research Society, Pittsburg, 1990.
[42] F. Candau, in: C.R. Safinya, S.A. Safran, P.A. Pincus (Eds.), Material Research Society Symposium Proceedings: Macromolecular Liquids, vol. 177, Materials Research Society, Pittsburgh, 1990.
[43] L. Motte, A. Lebrun, M.P. Pileni, Progr. Colloid Polym. Sci 89 (1992) 99.
[44] D. Ichinohe, T. Arai, H. Kise, Synth. Met. 84 (1997) 75.
[45] K.V. Schubert, K.M. Lusvardi, E.W. Kaler, Colloid Polym. Sci. 274 (1996) 875.
[46] F.M. Menger, K. Yamada, J. Am. Chem. Soc. 101 (22) (1979) 6731.
[47] D. Chatenay, W. Urbach, A.M. Cazabat, M. Vacher, M. Waks, Biophys. J. 48 (1985) 893.
[48] G.S. Timmins, M.J. Davies, B.C. Gilbert, H. Caldararu, J. Chem. Soc. Faraday Trans. 90 (18) (1994) 2643.
[49] A.V. Kabanov, Makromol. Chem. Macromol. Symp. 44 (1991) 253.
[50] V. Crupi, G. Maisano, D. Majolino, R. Ponterio, V. Villari, E. Caponetti, J. Mol. Struct. 383 (1996) 171.
[51] B. Bedwell, E. Gulari, in: K.L. Mittal (Ed.), Solution Behavior of Surfactants, vol. 2, Plenum Press, New York, 1982.
[52] E. Gulari, B. Bedwell, S. Alkhafaji, J. Colloid Interface Sci. 77 (1) (1980) 202.
[53] M. Zulauf, H.-F. Eicke, J. Phys. Chem. 83 (4) (1979) 480.
[54] H.-F. Eicke, in: I.D. Rob (Ed.), Microemulsions, Plenum Press, New York, 1982, p. 10.
[55] J.D. Nicholson, J.V. Doherty, J.H.R. Clarke, in: I.D. Rob (Ed.), Microemulsions, Plenum Press, New York, 1982, p. 33.
[56] H.-F. Eicke, J. Rehak, Helv. Chim. Acta 59 (8) (1976) 2883.
[57] P.D.I. Fletcher, B.H. Robinson, F. Bermejo-Barrera, D.G. Oakenfull, J.C. Dore, D.C. Steytler, in: I.D. Rob (Ed.), Microemulsions, Plenum Press, New York, 1982, p. 221.
[58] P.C. Cabos, P. Delord, J. Appl. Cryst. 12 (1979) 502.
[59] S. Radiman, L.E. Fountain, C. Toprakcioglu, A. de Vallera, P. Chieux, Progr. Colloid Polym. Sci. 81 (1990) 54.
[60] J.P. Huruguen, T. Zemb, M.P. Pileni, Progr. Colloid Polym. Sci. 89 (1992) 39.
[61] M.P. Pileni, T. Zemb, C. Petit, Chem. Phys. Lett. 118 (4) (1985) 414.
[62] W. Sager, W. Sun, H.-F. Eicke, Progr. Colloid Polym. Sci. 89 (1992) 284.
[63] S.A. Safran, G.S. Grest, A.L.R. Bug, in: H.L. Rosano, M. Clause (Eds.), Microemulsion Systems, Marcel Dekker, New York, 1987, p. 235.
[64] T.H. Wines, A.S. Dukhin, P. Somasundaran, Acoustic spectroscopy for characterizing heptane/H20/AOT reverse microemulsions. J. Coll. Interfce Sci. 216 (1999) 303–308.